

An asteroseismic signature of helium ionization

G. Houdek^{1*}, D. O. Gough^{1,2,3}

¹ *Institute of Astronomy, Madingley Road, Cambridge CB3 0HA, UK*

² *Department of Applied Mathematics and Theoretical Physics, Wilberforce Road, Cambridge CB3 0WA, UK*

³ *South African Astronomical Observatory, PO Box 9, Observatory 7935, South Africa*

29 October 2021

ABSTRACT

We investigate the influence of the ionization of helium on the low-degree acoustic oscillation frequencies in model solar-type stars. The signature in the oscillation frequencies characterizing the ionization-induced depression of the first adiabatic exponent γ is a superposition of two decaying periodic functions of frequency ν , with ‘frequencies’ that are approximately twice the acoustic depths of the centres of the He I and He II ionization regions. That variation is probably best exhibited in the second frequency difference $\Delta_2\nu_{n,l} \equiv \nu_{n-1,l} - 2\nu_{n,l} + \nu_{n+1,l}$. We show how an analytic approximation to the variation of γ leads to a simple representation of this oscillatory contribution to $\Delta_2\nu$ which can be used to characterize the γ variation, our intention being to use it as a seismic diagnostic of the helium abundance of the star. We emphasize that the objective is to characterize γ , not merely to find a formula for $\Delta_2\nu$ that reproduces the data.

Key words:

stars: abundances – stars: interior – stars: oscillations – Sun: abundances – Sun: oscillations.

1 INTRODUCTION

The issue addressed in this paper concerns the direct interpretation of an asteroseismic signature of helium ionization in terms of an ionization-induced property of the stratification of the star that produces that signature. The knowledge so obtained is important for designing calibrations of theoretical stellar models against seismic data (together with other astronomical data), for the purposes of obtaining estimates of some of the gross properties of stars, such as their ages and their chemical compositions.

The first approach that might come to mind is to adjust apparently appropriate parameters of the stellar models in such a way as to minimize some measure of deviation of the individual theoretical oscillation eigenfrequencies from the observed frequencies. Without careful regard to the extent to which those frequencies are influenced by the stellar properties in mind, namely the helium abundance Y in this discussion, this naive procedure can hardly be optimal, although it has been used: it was first carried out for the Sun, by Christensen-Dalsgaard & Gough (1981), who simply minimized the frequency misfit by least squares. The procedure has the merit of being simple to execute, but it is subject to all the uncertainties in stellar modelling, some of which need not necessarily be very pertinent to the ob-

jective of the calibration. It is more prudent to aim to work instead with certain combinations of frequencies that are insensitive to the irrelevant properties of the stellar modelling. Commonly used have been the so-called large and small frequency separations, which are relatively insensitive to the uncertain state of the outer layers of the stars (e.g. Christensen-Dalsgaard & Gough 1984; Gough 1986b). Christensen-Dalsgaard (1986, see also Ulrich 1986; Gough 1987) illustrated how from a knowledge of these separations one could in principle estimate the mass and age of a main-sequence star, provided that its chemical composition were known; indeed, in the early days of helioseismology these separations were often preferred to the raw frequencies for solar calibrations (Christensen-Dalsgaard & Gough 1980; Shibahashi, Noels & Gabriel 1983; Ulrich & Rhodes Jr 1983). But the chemical composition of a star, particularly the helium abundance, is often not well known, and it is therefore incumbent upon us to devise more reliable ways of determining it, especially in view of the high-precision data anticipated from the imminent space missions COROT (Convection Rotation and Planetary Transits; Baglin 2003) and Kepler (Borucki et al. 2003; Basri, Borucki & Koch 2005), and from the ground-based campaigns such as SONG (Grundahl et al. 2006) and those of the kind organized by Kjeldsen, Bedding and their colleagues (e.g. Kjeldsen et al. 2005). Even in the Sun, in which helium was discovered by J.N. Lockyer and P.J.C. Janssen in prominences observed during

* e-mail: hg@ast.cam.ac.uk

the eclipse of 1868, the spectroscopic determination of Y remains elusive to this day. This comes about because helium spectrum lines are formed well above the photosphere, in the much hotter chromosphere and corona where the deviation from local thermodynamic equilibrium can be severe, and where the helium abundance is not even necessarily the same as in the layers beneath the visible surface.

In principle, a direct seismological signature of Y in the envelope of a (sufficiently cool) star can be sought through its effect on the sound speed, via the depression of the value of the first adiabatic exponent γ induced by ionization, particularly if the depression occurs in an essentially adiabatically stratified region of a convection zone. The variation is seismically abrupt, in the sense that, at least for lower-frequency modes, its radial extent is less than or comparable with the inverse radial wavenumber of the eigenfunctions. We call such a feature an acoustic glitch. It causes a small shift in the eigenfrequencies, relative to those in a corresponding putative star with no ionization, that shift being an oscillatory function of the frequency itself. The amplitude of that function increases monotonically with Y , and should therefore be a robust indicator of the value of Y ; the frequency of the function is determined by the acoustic depth of the centre of ionization beneath the seismic surface of the star.

Oscillatory components are produced also by other acoustic glitches, such as that at the base of the convection zone which is caused by a near-discontinuity in the gradient of the density scale height. They are evident in the large separations $\Delta_1\nu_{n,l} \equiv \nu_{n,l} - \nu_{n-1,l}$ between the cyclic eigenfrequencies $\nu_{n,l}$ of seismic oscillations of order n and degree l , complicating the measurement of the underlying smooth component of $\Delta_1\nu_{n,l}$, and also of other diagnostics such as the small separation $\nu_{n,l} - \nu_{n-1,l+2}$. Not taking them into account leaves an undulation in the outcome of data-fitting when plotted against the extremities of the range of frequencies employed (Gough 2001), which could lead to misinterpretation. Therefore it is prudent to separate the smooth and the oscillatory components, using the two of them as complementary diagnostics. We address in this paper a way in which that separation could be carried out, by analysing signatures suggested by asymptotic analysis of the eigenfrequencies of a grid of solar models, with the intention of determining parameters that are good measures of the variation of the stratification in the second helium ionization zone that are not unduly contaminated by other properties.

Direct seismological signatures of the helium abundance in the solar interior have been constructed from intermediate-degree acoustic modes by various techniques (e.g. Gough 1984a; Däppen et al. 1991; Kosovichev et al. 1992; Vorontsov, Baturin & Pamyatnykh 1992; Pérez Hernández & Christensen-Dalsgaard 1994b; Basu & Antia 1995). In distant stars, however, only low-degree modes can be observed, and we need to find a diagnostic in only those modes, a need which has been stressed before by e.g. Gough (1990, 1998). One procedure is to attempt a direct inversion of low-degree modes for the helium abundance Y , using the constraint that the bulk of the convection zone is adiabatically stratified (Kosovichev 1993). More commonly, the outer phase function $\tilde{\alpha}(\omega)$ in the asymptotic relation

$$(n + \tilde{\alpha})\pi/\omega = \tilde{F}(w) + \dots \quad (1)$$

(Gough 1984b, 1993; Vorontsov 1988; Vorontsov, Baturin & Pamyatnykh 1991) has been used, for it exhibits explicitly the oscillatory components of ω induced by ionization (e.g. Baturin & Mironova 1990a,b; Christensen-Dalsgaard & Pérez Hernández 1992; Roxburgh & Vorontsov 1994); here ω is the angular frequency of a mode of order n and degree l , $w = \omega/(l + \frac{1}{2})$ and \tilde{F} is a function of w which depends also on the structure of the star. The idea is to determine $\tilde{\alpha}$ by fitting the functional form of its asymptotic relation to the seismic data (cf. Gough 1986a; Vorontsov 1988; Gough & Vorontsov 1995). It is evident from that relation that $\tilde{\alpha}/\omega$ (and $\pi^{-1}\tilde{F}$) can be determined from data $\omega_{n,l}$ only up to an unknown additive constant, so Brodsky & Vorontsov (1987) proposed using the derivative $\tilde{\beta} = d(\omega^{-1}\tilde{\alpha})/d\omega$, which contains the same information and is more elegant. The oscillatory component can be largely separated by appropriate filtering (cf. Pérez Hernández & Christensen-Dalsgaard 1994a), and the contribution from helium ionization used to calibrate stellar models to determine Y (e.g. Pérez Hernández & Christensen-Dalsgaard 1994b, 1998; Lopes et al. 1997; Lopes & Gough 2001).

An alternative procedure is to consider the second frequency difference, $\Delta_2\nu_{n,l}$ (Gough 1990), or even higher-order differences (Basu, Antia & Narasimha 1994; Basu 1997), which are much simpler to extract from the data than the phase functions $\tilde{\alpha}$ and $\tilde{\beta}$ yet appear to contain the same information. It has been found expedient to model their oscillatory components with parametrized functions derived from representations of the acoustic glitches, and then to determine the sought-for properties of the star by calibrating the parameters corresponding to a sequence of stellar models against the seismic data. Various approximate formulae for the seismic signatures that are associated with the helium ionization have been suggested and used, by Monteiro & Thompson (1998, 2005), Gough (2002), Miglio et al. (2003), Basu et al. (2004), Verner, Chaplin & Elsworth (2004) and Ballot, Turck-Chièze & García (2004), not all of which are derived directly from explicit acoustic glitches. Gough used an analytic function for modelling the dip in the first adiabatic exponent. In contrast, Monteiro & Thompson (1998) assumed a triangular form, which was adopted also by Monteiro & Thompson (2005), Miglio et al. and Verner et al. These are the only two attempts to relate the low-degree seismic signature directly to the properties of the ionization zone, although the latter appears to be too crude to capture the physics adequately (Monteiro & Thompson 2005). Basu et al. (2004), Ballot et al. (2004) and Piau, Ballot & Turck-Chièze (2005) have adopted a seismic signature for helium ionization that is similar to that arising from a single discontinuity in the sound speed (see also Basu, Antia & Narasimha 1994; Basu 1997), which is even less appropriate; the artificial discontinuities in the sound speed and its derivatives that this and the triangular representations possess cause the amplitude of the oscillatory signal to decay with frequency too gradually, although that deficiency may not be immediately noticeable within the limited frequency range in which adequate asteroseismic data are or will imminently be available. However, any inappropriate representation of the seismic signature can hardly be trusted to measure the characteristic of the glitch that causes it.

Although the seismic quantities $\tilde{\alpha}, \tilde{\beta}$ associated with low-degree modes and $\Delta_k \nu_{n,l}$ have been analysed in such a way as to enable the magnitude of the oscillatory components produced by helium ionization to be obtained, in none of the studies, save those of Monteiro & Thompson (1998, 2005) and Gough (2002), was the signature related directly to the form of the acoustic glitch that produced them. They were simply used as a medium for fitting theoretical models to seismic data, in the hope that the stellar properties of interest, such as Y , had been determined reliably. It has not been demonstrated whether the inferences are essentially uncontaminated by other properties of the star. Our aim in this paper is to design a seismic signature that truly reflects the properties of the seismic glitches we wish to measure. And we report below that we have been reasonably successful. The next step in advancing our understanding would require a further independent study of stellar structure (and the equation of state) to ascertain how the glitch properties relate to Y . The glitch amplitude increases with increasing Y . However, we have found that the rate at which it does so depends also on other factors, such as the entropy of the adiabatically stratified ionization zones, as has been noted previously by Däppen, Gough & Thompson (1988), Lopes et al. (1997) and Pérez Hernández & Christensen-Dalsgaard (1998), and that therefore the glitch amplitude alone is not a simple measure of Y .

In Sun-like stars, the stratification in the helium ionization zones is very close to being adiabatic (and Reynolds stresses are negligible), and consequently changes $\delta\gamma$ in γ produce well defined changes in the variation of sound speed with radius. We note, in passing, that the ionization of hydrogen produces much greater γ variation, but unfortunately (for this study) the hydrogen ionization zone is not even approximately adiabatically stratified throughout; the form of the seismic glitch must be susceptible to the uncertain formalism adopted to model the convective energy and momentum fluxes, and relating it to γ must therefore be unreliable. For that reason we concentrate on the ionization of helium, as have others before us. We represent the variation of γ with a pair of Gaussian functions. This correctly results in a decay of the amplitude of the seismic signature with oscillation frequency that is faster than that which the triangular and the single-discontinuity approximations imply, and also takes some account of the two ionization states of helium.

The plan of the paper is as follows: in the following Section we introduce and derive a simple seismic diagnostic of a Gaussian acoustic glitch produced by only the (dominant) second ionization of helium, together with a representation of the contribution from the base of the convection zone, the latter being derived in Appendix B; the variation of the eigenfunction phase ψ with acoustic depth τ is first represented by the simple formula $\psi \simeq \omega\tau + \epsilon$, where ϵ is taken to be constant. This diagnostic is tested against artificial frequency data computed from two sequences of theoretical solar models, which we describe in Section 3. Although the diagnostic can be fitted to the theoretical eigenfrequencies tolerably well, the inferred value of the acoustic depth τ_{II} of the glitch is too low, and the inferred amplitude $-\delta\gamma/\gamma|_{\tau=\tau_{\text{II}}}$ is too high. This is as one might expect, partly because in this initial phase of the investigation we have adopted only a single Gaussian function to represent the two ionization stages of helium, and partly because we have overestimated

$\psi(\tau_{\text{II}})$ by not taking account of the acoustic cutoff frequency ω_a . We rectify this, in two steps, in Section 4, first by incorporating ω_a into ψ , which essentially halves the discrepancy between the true τ_{II} and its seismologically inferred value, and also reduces the amplitude discrepancy considerably (although it does not reduce the measure χ^2 of the data misfit), and then by adding in a simple way a contribution to the diagnostic from the first stage of ionization of helium, which reduces the Δ_{II} discrepancy by a factor three (and also reduces χ^2). We must point out, however, that the value we must adopt for the ratio $\Delta_{\text{I}}/\Delta_{\text{II}}$ of the characteristic widths of the He I and He II glitches in order to obtain a good fit to the artificial data is rather larger than that suggested by the models. We do not know why, although a change of this kind is perhaps suggested by the functional form of the contribution to the depression of γ due to the ionization of hydrogen, which is depicted in Fig. 7. We discuss our analyses further in Section 5, and we draw our conclusions in Section 6.

2 THE SEISMIC DIAGNOSTIC

A convenient and easily evaluated measure of the oscillatory component is the second difference with respect to order n of the cyclic frequencies $\nu_{n,l}$ of like degree l :

$$\Delta_2 \nu_{n,l} \equiv \nu_{n-1,l} - 2\nu_{n,l} + \nu_{n+1,l}, \quad (2)$$

(Gough 1990). This measure is contaminated less than the first difference $\Delta_1 \nu_{n,l} \equiv \nu_{n,l} - \nu_{n-1,l}$, otherwise known as the large frequency separation, by the smoothly varying components of $\Delta_1 \nu$ (here and henceforth we simplify the notation, where it is not ambiguous to do so, by omitting the subscripts n, l). And it is less susceptible to data errors than the fourth and other higher-order differences (see Appendix C); moreover, adopting higher-order differences risks requiring more consecutive modes than might be available to provide a practical diagnostic.

Any localized region of rapid variation of the propagation speed of an acoustic wave, which here we call an acoustic glitch, induces an oscillatory component in $\Delta_2 \nu$ with a ‘cyclic frequency’ approximately equal to twice the acoustic depth

$$\tau = \int_{r_{\text{glitch}}}^R c^{-1} dr \quad (3)$$

of the glitch, where r is a radial coordinate, c is the adiabatic sound speed and R is the radius of the seismic surface of the star (essentially the surface on which c^2 , if extrapolated linearly outwards from the outer layers of the adiabatically stratified region of the convection zone, would vanish – cf. Balmforth & Gough 1990). The amplitude of the oscillatory component depends on the amplitude of the glitch, and decays with ν once the inverse radial wavenumber of the mode becomes comparable with or greater than the radial extent of the glitch. By calibrating a theoretical representation of the effect of glitches against the observations one can, in principle, learn about the characteristics of those glitches. Because only low-degree modes are used, the l -dependence can safely be ignored, even down to the base of the convection zone (except, possibly, in very-low-mass, almost fully convective stars). We remark further on that in Section 5. If a frame of reference exists in which the basic structure of

a star, which in general is presumed to be rotating (but only slowly), is independent of time, then one can seek linearized adiabatic oscillations in that frame whose time dependence is sinusoidal with angular frequency ω . The adiabatic oscillation frequency ω is related to the displacement eigenfunction ξ through a variational principle (Chandrasekhar 1963; Lynden-Bell & Ostriker 1967), the derivation of the acoustic signature from which we now address. We consider the structure of the star to be described by smoothly varying functions upon which are superposed glitches, each varying on a small spatial scale. The contribution $\delta\omega$ from those glitches to the eigenfrequency ω of a mode of oscillation (with vanishing pressure gradient at the surface), can then be written (see Appendix A)

$$\delta\omega \simeq \frac{\delta\mathcal{K} - \omega\delta\mathcal{I}}{2\omega\mathcal{I}}, \quad (4)$$

where \mathcal{I} is the mode inertia and $\delta\mathcal{K}$ depends on the displacement eigenfunction ξ and on the glitches in the equilibrium quantities, such as the (localized) perturbation $\delta\gamma$ to the first adiabatic exponent $\gamma = (\partial \ln p / \partial \ln \rho)_s$, s being specific entropy, caused by ionization. In equation (4), contributions from the surface (which at most contribute a relatively smoothly varying component to $\Delta_2\nu$) have been ignored.

We separate $\delta\omega$ into a smoothly varying component $\delta_{\text{sm}}\omega$ and an oscillatory component $\delta_{\text{osc}}\omega$:

$$\delta\omega = \delta_{\text{sm}}\omega + \delta_{\text{osc}}\omega, \quad (5)$$

(and we adopt a similar notation for other variables) and we approximate, with a suitable eigenfunction normalization, the oscillatory component $\delta_{\gamma,\text{osc}}\omega$ associated with helium ionization as follows:

$$\delta_{\gamma,\text{osc}}\omega = \text{osc}(\delta_{\gamma}\omega),$$

where

$$\delta_{\gamma}\omega := \frac{\delta_{\gamma}\mathcal{K}}{2\omega\mathcal{I}}, \quad (6)$$

with

$$\delta_{\gamma}\mathcal{K} \simeq \delta_{\gamma}\mathcal{K}_1 = \int (\delta\gamma) p (\text{div}\xi)^2 r^2 dr, \quad (7)$$

(cf. equations (A5), (A6)) and

$$\mathcal{I} = \int \rho \xi \cdot \xi r^2 dr, \quad (8)$$

the integrations being over the entire extent of the star, where p and ρ are pressure and density of the equilibrium state, and $\delta\gamma$ is a suitably defined rapidly varying perturbation to γ induced by ionization; *osc* denotes oscillatory part. We have confirmed numerically that the terms neglected in $\delta\mathcal{K}$ are indeed substantially smaller than $\delta_{\gamma}\mathcal{K}$ (although they may not be wholly negligible, as is evinced by the differences in $\delta\gamma/\gamma|_{\tau_{\text{II}}}$ in Figs 9 and 10). In view of the variational principle, we have approximated the eigenfrequencies by those of a corresponding nonrotating smoothly varying (i.e. having no glitches) model star; consequently in equations (7) and (8) we have been able to adopt the usual separation of the components of the eigenfunctions ξ in terms of functions of r and spherical harmonics, carry out the angular integrations, and regard ξ to be a function of r alone. In the asymptotic limit of high-order modes the (suitably normalized) radial component ξ of the displacement eigenfunction

ξ and the associated Lagrangian pressure perturbation \bar{p} are given by (e.g. Gough 1993)

$$\xi \simeq \frac{K^{1/2}}{r\rho^{1/2}} \cos\psi, \quad \bar{p} \simeq \frac{\omega^2\rho^{1/2}}{rK^{1/2}} \sin\psi, \quad (9)$$

where the phase function ψ is given by

$$\psi = \int_r^{r_t} K(r') dr' + \frac{\pi}{4} \simeq \omega\tau + \epsilon, \quad (10)$$

in which here we have approximated the radial component of the wavenumber of high-order modes as $K \simeq \omega/c$, and we have assumed that r is not close to r_t , the upper turning point at which the mode is reflected; ϵ is a phase constant (strictly speaking, a phase variable, for it varies slowly with ω , but in the simple approach that we adopt in just this section that variation is ignored) which takes some account of the fact that K deviates substantially from ω/c near the upper turning point. It follows that

$$(\text{div}\xi)^2 = \left(\frac{\bar{p}}{\gamma p}\right)^2 \simeq \frac{\omega^3}{\gamma p c r^2} \sin^2\psi, \quad (11)$$

and therefore equation (7) can be written in terms of

$$\delta_{\gamma,\text{osc}}\mathcal{K}_1 \simeq -\frac{1}{2}\omega^3 \int \frac{\delta\gamma}{\gamma} \cos 2(\omega\tau + \epsilon) d\tau, \quad (12)$$

in which the limits of integration are such as to include the region in which $\delta\gamma$ is nonzero; moreover

$$\mathcal{I} \simeq \omega \int_0^T \cos^2(\omega\tau + \epsilon) d\tau \simeq \frac{1}{2}T\omega, \quad (13)$$

where T is the acoustic radius of the star (i.e. the sound travel time from the acoustic surface to the centre of the star). Note that the normalization of this expression for the inertia differs from the usual. The neglect of the acoustic cutoff frequency in the expression for K will be dropped in Section 4.1. However, we shall continue to neglect the degree-dependence, which is a good approximation for the low-degree modes detectable by asteroseismology; we justify that neglect in Section 5.

In this introductory discussion we represent the acoustic glitch induced by the (second) ionization of helium by a Gaussian function about the acoustic depth $\tau = \tau_{\text{II}}$ of the centre of the He II ionization region (see Fig. 3), as did Gough (2002):

$$\frac{\delta\gamma}{\gamma} \simeq G(\tau; \Gamma_{\text{II}}, \tau_{\text{II}}, \Delta_{\text{II}}) \equiv -\frac{1}{\sqrt{2\pi}} \frac{\Gamma_{\text{II}}}{\Delta_{\text{II}}} e^{-(\tau - \tau_{\text{II}})^2 / 2\Delta_{\text{II}}^2}, \quad (14)$$

in which Γ_{II} and Δ_{II} are constants and Δ_{II} is much smaller than both τ_{II} and $T - \tau_{\text{II}}$. We improve on this simple expression in Section 4.2. The oscillatory component, $\delta_{\gamma,\text{osc}}\omega$, imparted by the glitch can then be estimated asymptotically from equations (6), (12) and (13) to be

$$\delta_{\gamma,\text{osc}}\omega \simeq A_{\text{II}}\omega e^{-2\Delta_{\text{II}}^2\omega^2} \cos 2(\tau_{\text{II}}\omega + \epsilon_{\text{II}}), \quad (15)$$

in which we have replaced the phase ϵ by ϵ_{II} , and we have introduced a normalized glitch amplitude

$$A_{\text{II}} = \frac{1}{2}\Gamma_{\text{II}}T^{-1}. \quad (16)$$

Notice that the amplitude of the oscillatory component $\delta_{\gamma,\text{osc}}\omega$ decays exponentially with ω^2 , which for large ω^2

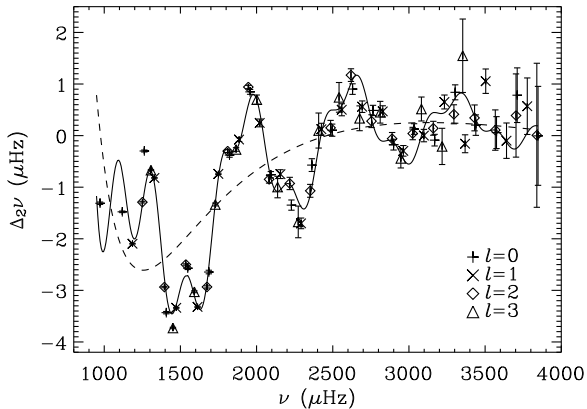


Figure 1. The symbols are second differences $\Delta_2\nu$, defined by equation (2), of low-degree solar frequencies obtained from GOLF data and kindly supplied by J. Ballot. Most of those data have been presented by Ballot et al. (2004). The most extreme outlying datum has been removed. The vertical bars represent standard data errors, evaluated under the assumption that the errors in the raw frequencies are independent; their effective overall value is $\langle\sigma\rangle = 4.3$ nHz. The curve is the seismic diagnostic $D_0(\nu; \alpha_k)$, which has been fitted to the data in a manner intended to provide an optimal estimate of the eleven parameters α_k . The values of some of those fitting parameters are: $-\delta\gamma/\gamma|_{\tau_{\text{II}}} = A_{\text{II}}/\sqrt{2\pi\nu_0\Delta_{\text{II}}} \simeq 0.065$, $\tau_{\text{II}} \simeq 707$ s, $\Delta_{\text{II}} \simeq 52$ s. The measure E of the overall misfit is 50 nHz. The direct measure $\bar{\chi}$ is 9.9; the minimum- χ^2 fit of the function D_0 to the data yields $\bar{\chi}_{\text{min}} = 7.0$.

is faster than the algebraic decay predicted by the representations of glitches containing discontinuities (cf. equation (17)); the amplitudes due to those perturbations decay only as ω^{-q} , where q is the order of the lowest derivative of a dynamically relevant variable of the equilibrium state that contains a discontinuity.

The acoustic glitch at the base of the convection zone ($r = r_c$) also contributes an oscillatory component, $\delta_{c,\text{osc}}\omega$, to the frequency ω of the modes, and hence to $\Delta_2\nu$. This component must be included when fitting functional forms for $\Delta_2\nu$ to real data, even though, in this investigation, our interest is restricted to helium ionization. The glitch is essentially a discontinuity in the acoustic cutoff frequency, and is reflected as a near discontinuity in $\partial\xi/\partial r$, but not in ξ (a local mixing-length model – as we have adopted in the construction of our theoretical test models – leads to a true discontinuity). From Appendix B we derive the following approximate expression (see equation (B19)):

$$\delta_{c,\text{osc}}\omega \simeq A_c\omega_0^3\omega^{-2} (1 + 1/4\tau_0^2\omega^2)^{-1/2} \times \cos[2(\tau_c\omega + \epsilon_c) + \tan^{-1}(2\tau_0\omega)], \quad (17)$$

with

$$A_c = \frac{c_c^2}{8\pi\omega_0^2} \left[\frac{d^2 \ln \rho}{dr^2} \right]_{r_c^-}^{r_c^+}, \quad (18)$$

where τ_c is the acoustic depth of the base of the convection zone and $c_c = c(r_c)$; $\tau_0 \ll T$ is a measure of the characteristic acoustic distance in the radiative interior over which the glitch causes the acoustic cutoff frequency to deviate substantially from a smooth function, and was determined

to be 80 s by fitting an exponential function to a theoretical reference solar model (see Appendix B). The (constant) quantity ω_0 is the asymptotic mean large frequency separation:

$$\omega_0 = \left(\frac{1}{\pi} \int_0^R c^{-1} dr \right)^{-1} = \frac{\pi}{T}, \quad (19)$$

which was determined from fitting by least-squares the asymptotic expression for the oscillation frequencies (e.g. Tassoul 1980; Gough 1986b) to the frequency data, namely

$$\nu_{n,l} \sim (n + \frac{1}{2}l + \varepsilon)\nu_0 - \frac{Bl(l+1) - C}{\nu_{n,l}} \nu_0^2, \quad (20)$$

in which $\nu_0 = \omega_0/2\pi$ and ε , B and C are also constants. The amplitude A_c is a measure of the discontinuity in the second derivative of ρ at the base of the convection zone. The amplitude factor $(1 + 1/4\tau_0^2\omega^2)^{-1/2}$ is only a weak function of ω , especially above cyclic frequencies of about 3 mHz in the solar case.

The amplitudes A_{II} and A_c , and the phase increments $2\epsilon_{\text{II}}$ and $2\epsilon_c + \tan^{-1}(2\tau_0\omega)$, vary only slowly with ω . This property facilitates the evaluation of the second differences of the oscillatory frequency perturbations given by equations (15) and (17), which is described in Appendix C, in which ϵ_{II} and ϵ_c are taken to be constants. Those constants cannot be taken to be the same because between τ_{II} and τ_c the relation $K = \omega/c$ is not exact. Indeed, this property also provides part of the reason why these constants cannot be written in terms of the phase ε appearing in the asymptotic eigenfrequency equation (20). Smooth contributions to the second differences of the eigenfrequencies (arising, in part, from refraction in the stellar core, from hydrogen ionization and from the superadiabaticity of the upper boundary layer of the convection zone which lies in an evanescent region of the acoustic mode) must also be accounted for. Guided by the functional form of the asymptotic relation (20), we approximate them by a third-degree polynomial in ω^{-1} . They account for both the second frequency differences of a putative reference solar model that has no glitches associated with helium ionization or the base of the convection zone, and the smooth contributions from those glitches. The complete fitting function is then given by

$$\Delta_2\nu \simeq \Delta_2(\delta_{\gamma,\text{osc}}\nu + \delta_{c,\text{osc}}\nu) + \sum_{k=0}^3 a_k\nu^{-k} \quad (21)$$

$$\begin{aligned} &\simeq F_{\text{II}}A_{\text{II}}\nu e^{-8\pi^2\Delta_{\text{II}}^2\nu^2} \cos[2(2\pi\tau_{\text{II}}\nu + \epsilon_{\text{II}}) - \delta_{\text{II}}] \\ &+ F_c A_c \nu_0^3 \nu^{-2} (1 + 1/16\pi^2\tau_0^2\nu^2)^{-1/2} \\ &\quad \times \cos[2(2\pi\tau_c\nu + \epsilon_c) + \tan^{-1}(4\pi\tau_0\nu) - \delta_c] \\ &+ \sum_{k=0}^3 a_k\nu^{-k} \equiv D_0(\nu; \alpha_k), \end{aligned} \quad (22)$$

where we have now converted to cyclic frequency ν , which we regard as a continuous variable; formulae for the amplitude factors F_{II} and F_c and for the phase increments δ_{II} and δ_c arising from taking the second differences are given by equations (C6) and (C7) with a and b given immediately following equation (C9) in the case of F_{II} and δ_{II} and by equations (C12) in the case of F_c and δ_c . The quantities α_k are the eleven parameters A_{II} , Δ_{II} , τ_{II} , ϵ_{II} , A_c , τ_c , ϵ_c and a_k ($k = 0, \dots, 3$).

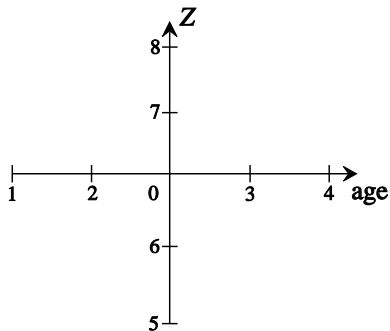


Figure 2. Denotation of the nine calibrated solar models which are used for testing the formulation of the second frequency differences. The ‘central model’ is model 0; the set of the four models (1-4) have a constant value of Z but varying age; the second set of the models (5-8) have constant age but varying Z .

In Fig. 1, second differences $\Delta_2\nu$ of solar oscillation frequencies obtained from the Global Oscillations at Low Frequency (GOLF) investigation on the Solar and Heliospheric Observatory (SOHO) spacecraft are plotted against ν . For comparison, the seismic diagnostic D_0 is plotted as a continuous curve against ν , which has been fitted to the data with the intention of providing an optimal estimate of the eleven parameters α_k by minimizing $E^2 = (\mathbf{D}_0 - \mathbf{d})^t \mathbf{C}^{-1} (\mathbf{D}_0 - \mathbf{d}) / \sum_k \lambda_k^{-1}$, where \mathbf{d} is the vector whose components are the N data $\Delta_2\nu_{n,l}$, \mathbf{D}_0 is the N -dimensional vector with components $D_0(\nu_{n,l}; \alpha_k)$, \mathbf{C} is the covariance matrix of the errors in the data \mathbf{d} , and the superscript t denotes transpose. The covariance matrix \mathbf{C} , whose eigenvalues are denoted by λ_k , was evaluated under the assumption that the errors in the measurements of the frequencies $\nu_{n,l}$ are independent random variables with variance $\sigma_{n,l}^2$; we take the square root of the harmonic mean of λ_k as an overall measure (σ) of the magnitude of the errors in the second differences. A direct measure of the fit of the curve to the data is given by $\bar{\chi}^2 = N^{-1} \sum_{n,l} \{ [D_0(\nu_{n,l}; \alpha_k) - \Delta_2\nu_{n,l}] / \sigma_{n,l} \}^2$.

A similar comparison may be made with comparable second differences of frequencies obtained from the Michelson Doppler Imager (MDI), also on SOHO, which, over the available frequency range, 1473–3711 μHz , of those data (from which, for equity, we have also removed the most extreme outlier) have overall error $\langle \sigma \rangle = 5.3 \text{ nHz}$, and deviate from the fitted diagnostic (22) by $E = 32 \text{ nHz}$, compared with $\langle \sigma \rangle = 6.4 \text{ nHz}$ and $E = 34 \text{ nHz}$ for the GOLF data over the same frequency range. The sharp upturn of the purported ‘smooth’ contribution (dashed curve) in Fig. 1 as ν decreases below 1300 μHz is probably an artefact of the failure of the asymptotic approximation upon which equation (22) is founded; this deficiency is removed partially by the improved diagnostic D_2 which we introduce in Section 4.

One should expect equation (22) to represent the second differences of the actual frequencies more faithfully than the expressions that have been used before (e.g., Monteiro & Thompson 1998, 2005; Gough 2002; Basu et al. 2004). This is so partly because here we use a representation of the HeII glitch in γ that is more realistic than the non-analytic functions adopted by Monteiro et al. and Basu et al., and we also use a more realistic representation of the stratification immediately beneath the convection zone.

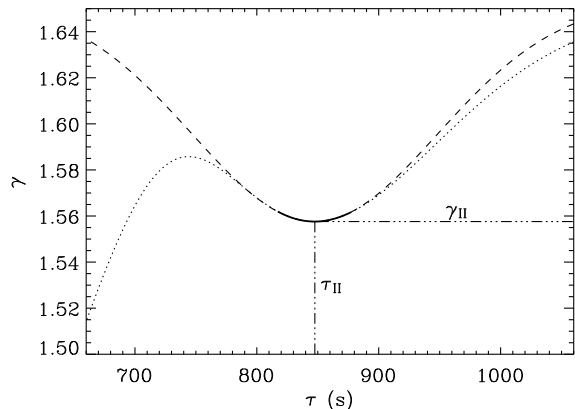


Figure 3. Adiabatic exponent γ (solid and dotted curve) for the central stellar model 0 as a function of the acoustic depth τ , which is measured from the acoustic surface of the model (estimated as the place where the linear extrapolation of c^2 from the region of the upper turning points of the modes vanishes, some 225 s above the photosphere). The dashed curve is $\gamma_{\text{II}0} - (\gamma_{\text{II}0} - \gamma_{\text{II}}) \exp[-(\tau - \tau_{\text{II}})^2 / 2\Delta_{\text{II}}^2]$, where $\gamma_{\text{II}0} = 1.651$ is the value of $\gamma(p(\tau_{\text{II}}), \vartheta(\tau_{\text{II}}), 0)$, evaluated at $Y = 0$ (dot-dashed curve in Fig. 7) and ϑ is temperature; the remaining parameters (γ_{II} , τ_{II} , Δ_{II}) have been adjusted to fit γ in the region in which the curve representing γ is solid, namely $\tau_{\text{II}} - \tau_{\text{f}} < \tau < \tau_{\text{II}} + \tau_{\text{f}}$ with $\tau_{\text{f}} \simeq 30 \text{ s}$. The parameter γ_{II} is the minimum value of γ in the HeII ionization zone, and τ_{II} is the acoustic depth at that minimum. The parameters associated with the other test models were determined likewise, with values of τ_{f} as close as possible to that of the central model subject to their fitting exactly onto the computational mesh; their values differ from that of the central model by less than 3 s.

3 TESTING THE FORMULATION ON THEORETICAL MODELS

3.1 Test models

Two sets of five calibrated evolutionary models for the Sun were used. The models had been computed by Gough & Novotny (1990) using the procedure described by Christensen-Dalsgaard (1981). The opacity values were obtained from interpolating in the Los Alamos Opacity Library for the Grevesse (1984) mixture, supplemented at low temperature by interpolating in the tables of Cox & Stewart (1970a,b). Gravitational settling was not included. One set of models has a constant value for the heavy-element abundance Z but varying age in (logarithmically) uniform steps of magnitude approximately 0.051 in $\ln t$ (t being age); the other has constant age but varying Z , in uniform steps of magnitude approximately 0.016 in $\ln Z$. The central models (model 0, see Fig. 2) of the two sets coincide, having $t = 4.60 \text{ Gy}$ and $Z = 0.02014$. All models were calibrated by adjusting the initial helium abundance Y_0 and the mixing-length parameter to satisfy the solar values of the luminosity and photospheric radius: $L_{\odot} = 3.845 \times 10^{33} \text{ erg s}^{-1}$ and $R_{\odot} = 6.9626 \times 10^{10} \text{ cm}$, resulting in a central model with $Y_0 = 0.2762$. The models were examined carefully and adjusted to satisfy hydrostatic equilibrium to high precision. Eigenfrequencies of adiabatic oscillation modes with $l \leq 2$ were computed for all models in the Cowling approximation

(gravitational forces are long-range and do not materially affect glitch diagnostics, so the Cowling approximation is quite adequate for our purposes) using the *Aarhus Adiabatic Pulsation Package*¹. From these were constructed second frequency differences according to equation (2).

3.2 Test results

For all nine test models we determined the properties of the He II depression in γ by fitting a Gaussian (plus a constant) to γ . Details of this fitting process are illustrated in Fig. 3 for the central model 0. The three parameters, $-\delta\gamma/\gamma|_{\tau_{\text{II}}}$, τ_{II} and Δ_{II} so determined are plotted in the top three panels of Fig. 4 for the nine test models as a function of the helium abundance Y , where $-\delta\gamma/\gamma|_{\tau_{\text{II}}} \equiv 2(\gamma_{\text{II}0} - \gamma_{\text{II}})/(\gamma_{\text{II}0} + \gamma_{\text{II}})$. The value of $\gamma_{\text{II}0}$ is the value of γ evaluated with the pressure and temperature of the model at $\tau = \tau_{\text{II}}$, but with a helium abundance $Y = 0$ (see dotted curve in Fig. 7). For the central model $\gamma_{\text{II}0} = 1.651$. The values of the other models differ from that of the central model by less than 2×10^{-4} .

The first two lower panels in Fig. 4 display the value of A_c (equation (18)) and the acoustic depth τ_c of the base of the convection zone. These values were obtained by fitting analytical functions (as discussed by Christensen-Dalsgaard, Gough & Thompson 1991) to the first logarithmic density derivative, $d \ln \rho / d \ln r$, of the models either side of the discontinuity at the base of the convection zone, as explained in Appendix D. The third (rightmost) panel is a standard measure (mean squared residuals) χ^2 for the goodness of the Gaussian fit to the He II depression in γ .

The asymptotic formula D_0 was then fitted to the second differences of the computed eigenfrequencies of the models as described in Section 2; some of the resulting parameters are plotted in Fig. 5. There is a superficial resemblance to the corresponding direct estimates from the models depicted in Fig. 4 (except for the slope of $\Delta_{\text{II}}(Y)$ for the Z -varying sequence, which we suspect is influenced substantially by heavy-element ionization, and, of course, χ^2 , which has quite different meanings in the two figures). Perhaps the most obvious other difference is that the slopes of the $\delta\gamma/\gamma|_{\tau_{\text{II}}}$ curves from the two sequences of direct model measurements are almost the same, whereas those of the frequency-fitting are not. The magnitudes of the values of some of the parameters are also discrepant. As will become evident in Section 4, that is to be expected in the case of the parameters characterizing the ionization, partly because the seismological fit is influenced by the effect of He I ionization, which has been treated erroneously as being part of He II. The acoustic depths of the bases of the convection zones agree reasonably well. But the amplitudes do not; we do not know why.

4 FURTHER IMPROVEMENTS

4.1 Improved treatment of the asymptotic phase function ψ

One of the obvious deficiencies of our introductory analysis described in the previous section is our treatment of the

phase function ψ , which we approximated by $\psi \simeq \omega\tau + \epsilon$, neglecting the acoustic cutoff frequency ω_a (and also the relatively small horizontal component of the wavenumber) in evaluating the vertical component K of the wavenumber, whose full planar form is given by equation (B2). In this section we account for the effect of the frequency dependence of the upper turning point by keeping ω_a :

$$K(r) \simeq \frac{\omega}{c} \left(1 - \frac{\omega_a^2}{\omega^2} \right)^{1/2}, \quad (23)$$

representing the stratification of the outer stellar layers locally by a polytrope of index m , for which the acoustic cutoff frequency associated with the Lagrangian pressure perturbation (and corrected for the singularity at the top of the polytropic envelope – see Gough 1993) is

$$\omega_a = (m + 1)/\tau. \quad (24)$$

Thus, recognizing that the acoustic glitch associated with the helium ionization is confined to a small range of acoustic depth, we expand the phase function $\psi(\tau)$ about the (phase-shifted) centre of the glitch, $\tau = \tilde{\tau}_{\text{II}}$, having accommodated the phase constant ϵ_{II} by replacing $\omega\tau_{\text{II}}$ by $\omega\tilde{\tau}_{\text{II}} = \omega\tau_{\text{II}} + \epsilon_{\text{II}}$, yielding

$$\psi(\tau) \simeq \psi(\tilde{\tau}_{\text{II}}) + \omega\kappa_{\text{II}}(\tau - \tilde{\tau}_{\text{II}}) + \text{O}[(\tau - \tilde{\tau}_{\text{II}})^2], \quad (25)$$

with $\kappa_{\text{II}} = \kappa(\tilde{\tau}_{\text{II}})$, where

$$\kappa(\tau) \equiv \sqrt{1 - \left(\frac{m+1}{\omega\tau} \right)^2}. \quad (26)$$

We adopt $m = 3.5$ for all models; it was obtained from the slope of $1/\omega_a(\tau)$ in the outer layers of the adiabatically stratified region of the convection zone in the central model, and relating that to m using equation (24). We note, in passing, that this value is close to 3.0, the effective value of m in the region of the upper turning points of solar modes of intermediate degree determined by calibrating the asymptotic eigenfrequency formula (1) against observation (e.g. Christensen-Dalsgaard et al. 1985); actually, the values of χ^2 of the data-fits that follow are reduced somewhat if the value 3.5 is replaced by 3.0, but then the overestimates of corresponding values of the amplitudes $-\delta\gamma/\gamma|_{\tau_{\text{II}}}$ are greater. Taking expansion (25) to higher order makes a correction of magnitude typically less than one per cent, so we keep only these first two terms. The leading term in the expansion (25) is given by

$$\begin{aligned} \psi(\tilde{\tau}_{\text{II}}) &\simeq \omega \int_{\tilde{\tau}_{\text{II}}}^{(m+1)/\omega} \kappa \, d\tau + \frac{\pi}{4} \\ &= \kappa_{\text{II}} \tilde{\tau}_{\text{II}} \omega - (m+1) \cos^{-1} \left(\frac{m+1}{\tilde{\tau}_{\text{II}} \omega} \right) + \frac{\pi}{4}. \end{aligned} \quad (27)$$

The analysis proceeds as in Section 2 and Appendix A. The outcome is to change the inertia \mathcal{I} to

$$\begin{aligned} \mathcal{I} &\simeq \psi(T) - \frac{\pi}{4} \simeq \frac{1}{2} T \omega - \frac{1}{4} (m+1) \pi \\ &\simeq \frac{\pi \nu^2}{2\nu_0} \left[\nu + \frac{1}{2} (m+1) \nu_0 \right]^{-1}. \end{aligned} \quad (28)$$

The contribution to ν from the glitch then becomes

$$\delta\gamma\nu \simeq A_{\text{II}} \kappa_{\text{II}}^{-1} \left[\nu + \frac{1}{2} (m+1) \nu_0 \right] \left[e^{-8\pi^2 \kappa_{\text{II}}^2 \Delta_{\text{II}}^2 \nu^2} \cos(2\psi_{\text{II}}) - 1 \right], \quad (29)$$

¹ <http://astro.phys.au.dk/~jcd/adipack.n>

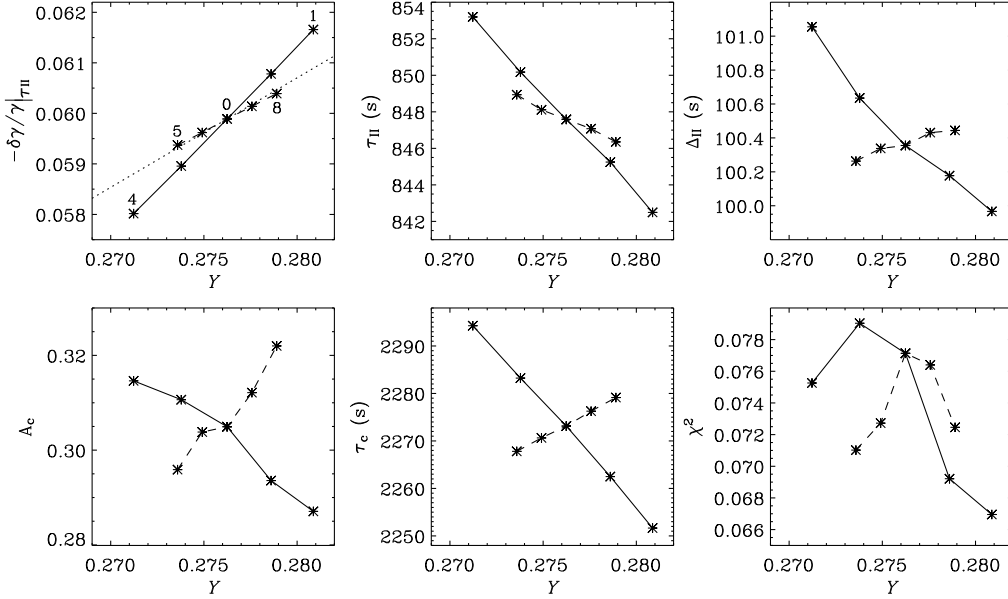


Figure 4. The top panels show $-\delta\gamma/\gamma|_{\tau_{\text{II}}} := 2(\gamma_{\text{II0}} - \gamma_{\text{II}})/(\gamma_{\text{II0}} + \gamma_{\text{II}})$, τ_{II} and Δ_{II} , which were determined from fitting a Gaussian (see Fig. 3) to the HeII depression in γ , for all nine test models, plotted against helium abundance Y . Models with varying age and constant heavy element abundance Z are connected with solid lines; models with varying Z and constant age are connected with dashed lines. The central model 0 and the models 1, 4, 5 and 8 are indicated in the upper left panel. Also in the upper left panel is a dotted straight line from the origin through the central model; it is evident that the effective amplitude of the helium-induced acoustic glitch is consistent with it being a linear function of Y in the Z -varying sequence, but not strictly so in the sequence with varying age. The lower right panel is the standard measure χ^2 (normalized integral of squared residuals: $\chi^2 = (2\Delta_{\text{II}})^{-1} \int (\delta\gamma/\gamma - G)^2 d\tau$, in which the integral is evaluated from $\tau_{\text{II}} - \Delta_{\text{II}}$ to $\tau_{\text{II}} + \Delta_{\text{II}}$) of the goodness of the fit between γ and the calibrated Gaussian. The first two lower panels show the properties of the density discontinuity (amplitude A_c and acoustic depth τ_c) at the base of the convection zone, which were determined from the equilibrium models.

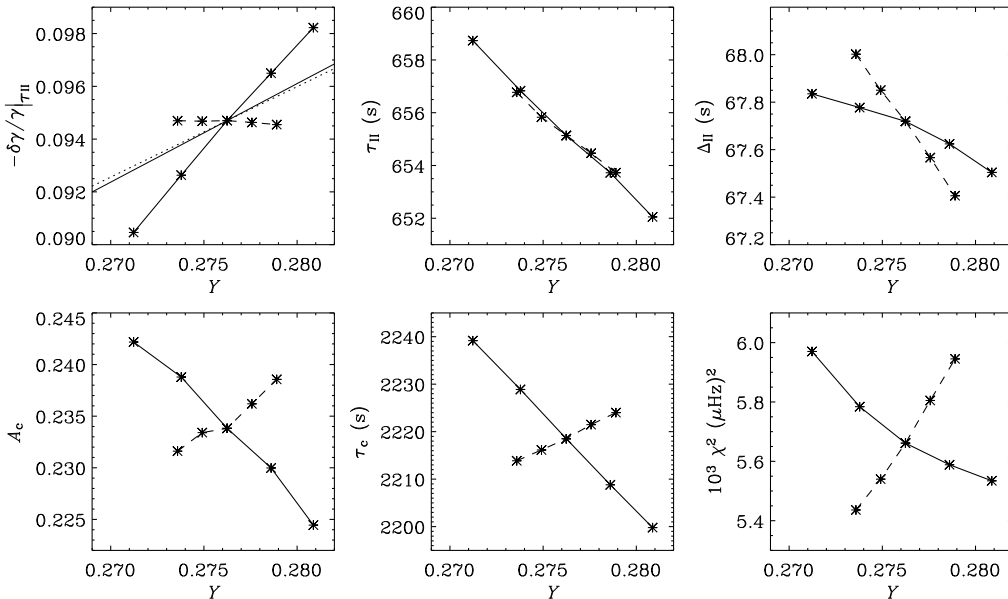


Figure 5. Model properties $-\delta\gamma/\gamma|_{\tau_{\text{II}}} = A_{\text{II}}/\sqrt{2\pi\nu_0\Delta_{\text{II}}}$, τ_{II} , Δ_{II} , A_c and τ_c for all nine test models determined from the diagnostic D_0 defined by equation (22). The fitting parameters A_{II} , τ_{II} , Δ_{II} , ϵ_{II} , A_c , τ_c and ϵ_c have been adjusted to fit the second differences $\Delta_2\nu$, defined by equation (2), of the low-degree ($l=0,1,2$), adiabatically computed, model eigenfrequencies. Note that the inferred values of $-\delta\gamma/\gamma|_{\tau_{\text{II}}}$ actually decrease, gradually, with increasing Y in the Z -varying sequence. The frequency range used in the least-squares fitting is that available to the BiSON data, with which we compare our final diagnostic formula in Fig. 12: it is 1322–4058 μHz . The lower right panel is the standard measure χ^2 (mean squared residuals, in units of $(\mu\text{Hz})^2$) of the goodness of the fit between $\Delta_2\nu$ of the modelled frequencies and the calibrated diagnostic. The line styles are as in Fig. 4. The dotted line in the upper left panel is again a straight line from the origin; for comparison the thin solid line is drawn with the same slope as the age-varying sequence in Fig. 4.

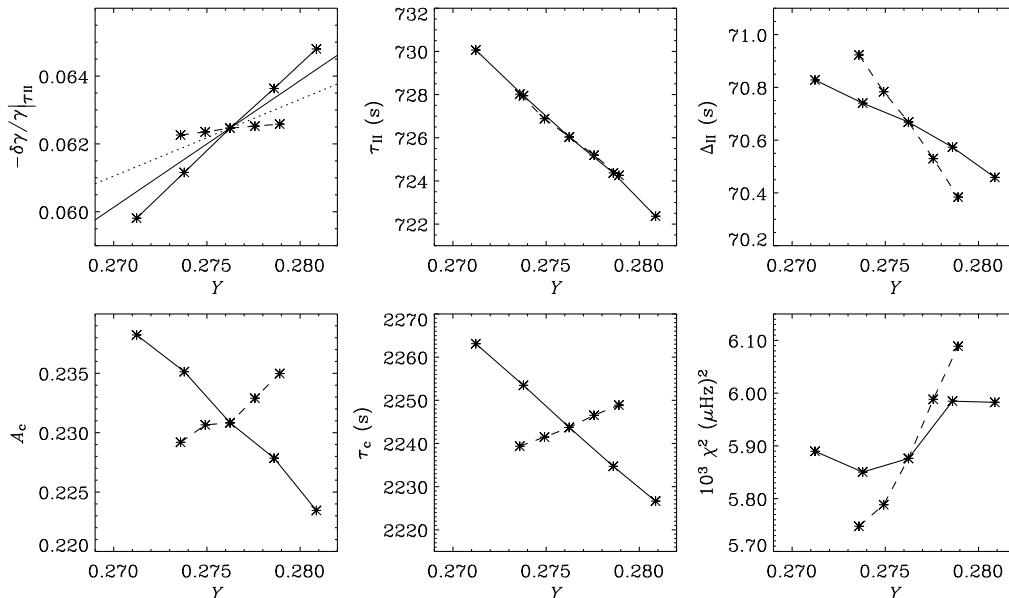


Figure 6. Model properties $-\delta\gamma/\gamma|_{\tau_{\text{II}}}$, τ_{II} , Δ_{II} , A_c and τ_c determined from the diagnostic D_1 defined by equations (21), (29) & (30) which includes an improved treatment of the phase function ψ given by equation (27). Results are shown for the nine test models. The fitting parameters A_{II} , τ_{II} , Δ_{II} , ϵ_{II} , A_c , τ_c and ϵ_c have been adjusted to fit the second differences $\Delta_2\nu$, defined by equation (2), of the low-degree ($l=0,1,2$), adiabatically computed, model frequencies. The smallest frequency value used in the least-squares fitting is $\nu \simeq 1322 \mu\text{Hz}$, the largest is $4058 \mu\text{Hz}$. The lower right panel is the standard measure χ^2 (mean squared residuals, in units of $(\mu\text{Hz})^2$) of the goodness of the fit between $\Delta_2\nu$ of the modelled frequencies and the calibrated diagnostic. The line styles are as in Fig. 4. The dotted line in the upper left panel is a straight line from the origin; the thin solid line is drawn with the same slope as the age-varying sequence in Fig. 4.

in which A_{II} is still given by equation (16), and $\psi_{\text{II}} = \psi(\tilde{\tau}_{\text{II}})$, with $\psi(\tilde{\tau}_{\text{II}})$ given by equation (27). The effect on the oscillatory component $\delta_{\gamma, \text{osc}}\nu$ is both to modify the amplitude of the cosine in equation (15) and effectively to impart an additional frequency-dependent contribution to the phase.

Beneath the convection zone the ω_a correction is small, and can be ignored; for the Sun, for example, $1 - \kappa(\tau) < 1 \times 10^{-2}$ for $\tau \geq \tau_c$. Moreover, the measure \mathcal{I}_{Ψ} of the inertia, introduced in Appendix B, is unchanged. Consequently the contribution from the acoustic glitch at the base of the convection zone is influenced significantly by ω_a only through the phase $\psi_c = \psi(\tilde{\tau}_c)$, where $\omega\tilde{\tau}_c = \omega\tau + \epsilon_c$, leading to

$$\delta_c\nu \simeq A_c\nu_0^3\nu^{-2} (1 + 1/16\pi^2\tau_0^2\nu^2)^{-1/2} \times \left\{ \cos[2\psi_c + \tan^{-1}(4\pi\tau_0\nu)] - (16\pi^2\tau_0^2\nu^2 + 1)^{1/2} \right\}, \quad (30)$$

where A_c is given by equation (18) and ψ_c by equation (B20).

The improved diagnostic function $D_1(\nu; \alpha_k)$ for representing the second frequency differences associated with the acoustic glitches is then given by equation (22) with the first term modified according to the oscillatory component of equation (29) and the second term by equation (30), and still with F_{II} and δ_{II} defined by equations (C6) and (C7) but with the extended expressions for α , a and b given by equations (C10) and (C11). The form of the seismic diagnostic from the base of the convection zone is unaffected, save for the replacement of $2\pi\tau_c\nu + \epsilon_c$ by ψ_c .

Results for the seismic diagnostic D_1 are shown in Fig. 6 for all nine test models (in which we have, as before, considered the smooth terms – i.e. the last terms in both equations (29) & (30) – to have been incorporated into the polynomial

in ν^{-1}). Compared with the results of the previous section, plotted in Fig. 5, the amplitudes $-\delta\gamma/\gamma|_{\tau_{\text{II}}}$ are smaller and the values of τ_{II} , Δ_{II} and τ_c are larger, all being closer to the model values depicted in Fig. 4.

4.2 Including He I ionization

A second deficiency in our initial procedure is that we took no explicit account of the first ionization of helium. The reason is that He I ionization is merged with the ionization of hydrogen, which dominates in the depression of γ even at the centre of He I ionization. However, the effect of the first ionization of helium is, as is evident in Fig. 7, not negligible; it broadens the hydrogen-induced dip in γ . Without precise knowledge of the hydrogen-induced profile (perhaps even with it) seismological calibration of the broadening is difficult. Our approach is not even to try. Instead we simply attempt to relate directly the reduction of γ by He I ionization to that due to He II ionization, which we do aim to measure. The much greater effect of hydrogen ionization is, on the whole, acoustically shallower than the effect of He I, and therefore produces a smoother seismic signal, and we trust that it is adequately accommodated by the polynomial $\sum a_k\nu^{-k}$ in the expression (21) for $\Delta_2\nu$.

The degree of helium ionization, and its effect on γ , is determined by the law of mass action for ionizing species, which is approximated by Saha-like equations (we use the approximate equation of state of Eggleton, Faulkner & Flannery 1973). It depends not only on the temperature and the number density of helium, but also on the free-electron

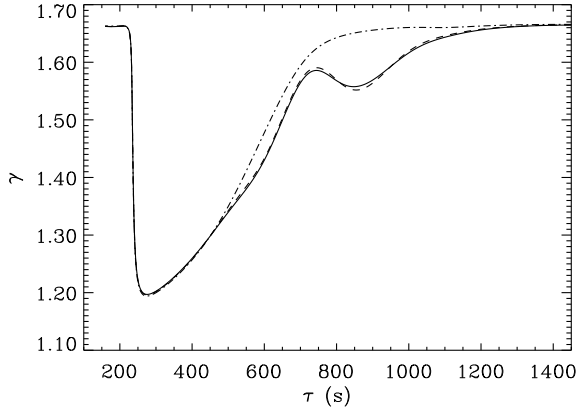


Figure 7. The solid curve is the adiabatic exponent $\gamma(p, \vartheta, Y)$, where ϑ is temperature, through the ionization zone of the central model 0; the dot-dashed curve is the adiabatic exponent $\gamma(p, \vartheta, 0)$. The dashed curve is the sum of the first two terms of the Taylor expansion of γ about $Y = 0$ given by equation (31). Note that the amplitude of variation of the dashed curve in the He II ionization zone is greater than that of the solid curve; the difference contributes to the discrepancy between the values of $\delta\gamma/\gamma|_{\tau_{\text{II}}}$ in Figs 9 and 10.

density, which itself depends on the abundances of all ionized species, especially hydrogen. In general these factors are nonlinearly dependent on one another, but we base our procedure here on the idea that because the number density of helium is quite low, although not extremely low, the influence on γ is approximately a linear function of the helium abundance Y . As we demonstrate below, the linear approximation works quite well, although it is evident from the top left panels of Figs 4, 5, 6, 9 and 10 that the linear approximation is not strictly correct. It is important to realize, however, that it is used solely for estimating the He I contribution to γ relative to the larger He II contribution, and therefore plays only a minor role in calibrating Y : our expectation is that it can account adequately for the deviation of the form of the seismic helium signature from those implied by the simple equations (15) and (29), thereby producing a more faithful match with the data, and consequently permitting a more robust calibration of the models against the star.

We first consider γ to be Taylor-expanded about $Y = 0$ in a reference stellar model, yielding

$$\gamma(\tau, Y) \simeq \gamma(\tau, 0) \Big|_{Y=0} + \frac{\partial\gamma}{\partial Y} \Big|_{Y=0} Y, \quad (31)$$

where the coefficients γ and $\partial\gamma/\partial Y$ on the right-hand side of equation (31) are evaluated at the temperature and pressure of the reference model but with $Y = 0$. We hold temperature, ϑ , rather than density, fixed under differentiation, because ionization depends much more sensitively on ϑ . We do not take heavy elements explicitly into account here because $\partial\gamma/\partial Z|_{Z=0}$, where Z is the total heavy element abundance, is rather smaller in magnitude than $\partial\gamma/\partial Y|_{Y=0}$, and in any case Z itself is much smaller than Y .

The variation $\delta\gamma$ in the adiabatic exponent γ induced by helium ionization then becomes:

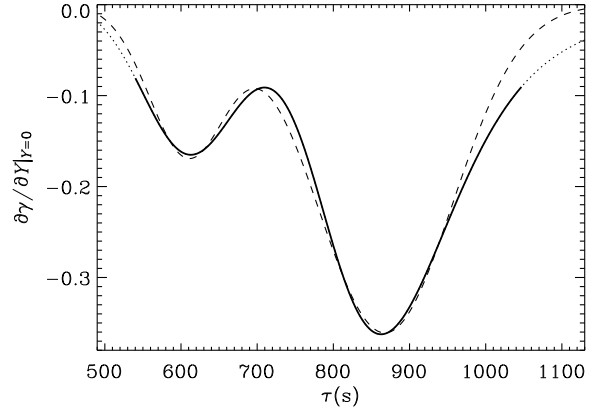


Figure 8. The solid and dotted curve is $\partial\gamma/\partial Y|_{Y=0}$ for the central model 0, the derivative being taken at constant p and ϑ (and Z). The dashed curve is the sum of the two Gaussian functions used in the construction of the seismic diagnostic (37) whose parameters have been adjusted to fit $\partial\gamma/\partial Y|_{Y=0}$ in the region in which the curve is solid.

$$\delta\gamma \simeq \frac{\partial\gamma}{\partial Y} \Big|_{Y=0} Y. \quad (32)$$

The first-order expansion (31) is illustrated in Fig. 7 for the central model 0; the solid curve denotes the adiabatic exponent $\gamma(p, \vartheta, Y)$ of the model, the dotted curve is $\gamma(p, \vartheta, 0)$, and the dashed curve is the right-hand side of equation (31). A plot of $\partial\gamma/\partial Y|_{Y=0}$ is presented in Fig. 8, also for the central model 0 (solid and dotted curve), which clearly exhibits the two glitches induced by He I and He II ionization, and which we formally represent by the sum of two Gaussian functions about the acoustic depths $\tau = \tau_{\text{I}}$ (He I) and $\tau = \tau_{\text{II}}$ (He II):

$$\frac{\partial\gamma}{\partial Y} \Big|_{Y=0} \simeq -\frac{\gamma}{\sqrt{2\pi}Y} \left[\frac{\Gamma_{\text{I}}}{\Delta_{\text{I}}} e^{-(\tau-\tau_{\text{I}})^2/2\Delta_{\text{I}}^2} + \frac{\Gamma_{\text{II}}}{\Delta_{\text{II}}} e^{-(\tau-\tau_{\text{II}})^2/2\Delta_{\text{II}}^2} \right], \quad (33)$$

in which γ and Y are the actual values in the original model. The dashed curve in Fig. 8 is a least-squares fit of the two Gaussian functions to $\partial\gamma/\partial Y|_{Y=0}$ of the central stellar model 0.

The fitting parameters for the nine reference models are illustrated in Fig. 9. Note that the ratios $\beta = \Gamma_{\text{I}}\Delta_{\text{II}}/\Gamma_{\text{II}}\Delta_{\text{I}}$, $\eta = \tau_{\text{I}}/\tau_{\text{II}}$ and $\mu = \Delta_{\text{I}}/\Delta_{\text{II}}$ hardly vary. Indeed, they vary at most by about 35% amongst adiabatically stratified model envelopes whose masses and radii vary by factors of five. Therefore, for the purpose of including He I ionization, we regard them as being constant. We adopt the values $\beta = 0.45$ and $\eta = 0.7$. But as is the case of several of the other parameters, particularly Δ_{II} , we have found that the value of μ that gives the best fit to the frequency data is not the same as the one that we have attempted to measure directly from the models. This is no doubt a result of contamination by hydrogen ionization, and perhaps ionization of heavy elements too. So instead we have adopted $\mu = 0.90$ for all models, which gives an optimal fit.

The asymptotic evaluation of the contribution to $\delta\omega$ from He I ionization proceeds analogously to the treatment of He II, except that now one must recognize that for low-frequency modes the upper turning point $\tau = \tau_{\text{e}}$ can be

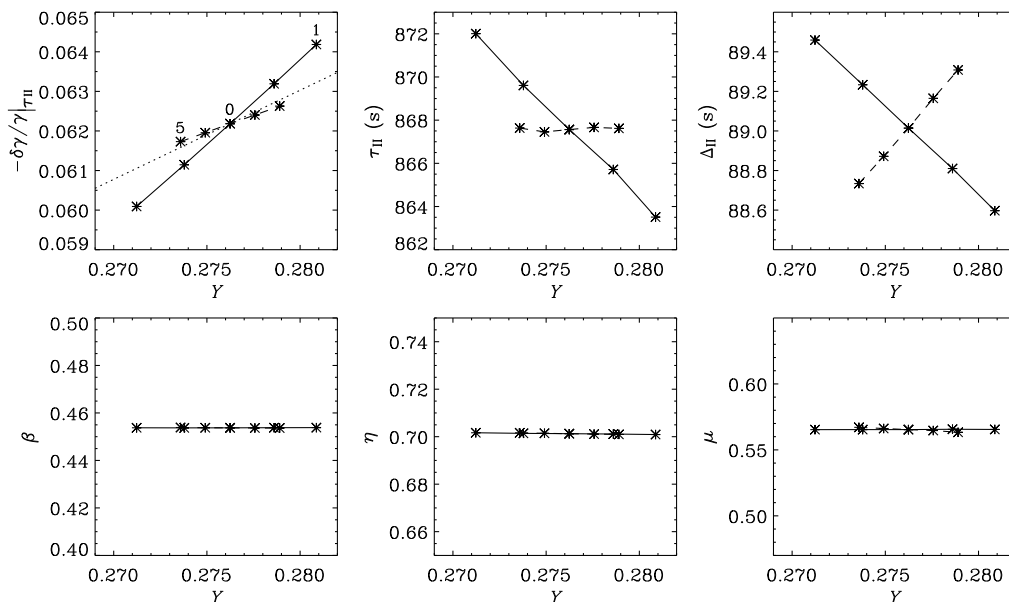


Figure 9. Properties of the HeII depression in γ for all nine test models as a function of Y . The HeII properties (top panels), including τ_{II} , were obtained from fitting the two Gaussians (equation (33)) to $\partial\gamma/\partial Y|_{Y=0}$ of the nine test models; they are somewhat greater than the acoustic depths of the minima in γ plotted in Fig. 4, apparently because the locations of those minima are influenced by the τ -dependent contribution from the hydrogen ionization. Partly as a consequence of fitting the Gaussians over an extended range of τ , the values of $-\delta\gamma/\gamma|_{\tau_{\text{II}}}$, which were computed according to equation (32), are somewhat greater than those in Fig. 4, possibly the result of a contribution from the ionization of the heavy elements; however, the difference is not great (cf. Fig. 7). The values (not plotted here) of A_c and τ_c are, of course, the same as those in Fig. 4. The line styles are as in Fig. 4. Also in the upper left panel is a dotted straight line from the origin through the central model; the effective amplitude of the helium-induced acoustic glitch is consistent with it being a linear function of Y in the Z -varying sequence, but not strictly so in the sequence with varying age. The lower panels show the values of β , η and μ .

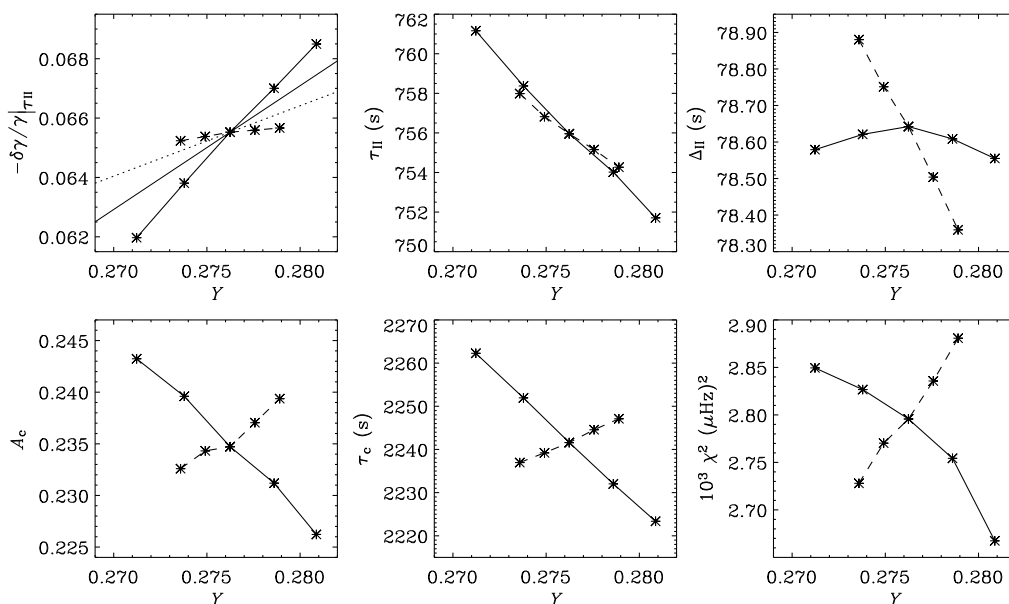


Figure 10. Model properties $-\delta\gamma/\gamma|_{\tau_{\text{II}}}$, defined as in Fig. 5, τ_{II} , Δ_{II} , A_c and τ_c determined from the seismic diagnostic D_2 defined by equations (21), (30) & (37), which includes a description for both the HeI and the HeII ionization zones. Results are displayed for the nine test models. The fitting parameters A_{II} , τ_{II} , Δ_{II} , ϵ_{II} , A_c , τ_c and ϵ_c have been adjusted to fit the second differences $\Delta_2\nu$, defined by equation (2), of the low-degree ($l=0,1,2$), adiabatically computed, model frequencies. The smallest frequency value used in the least-squares fitting is $\nu \simeq 1322 \mu\text{Hz}$, the largest is $4058 \mu\text{Hz}$. The lower right panel is the standard measure χ^2 of the goodness of the fit between $\Delta_2\nu$ of the modelled frequencies and the calibrated seismic diagnostic. The line styles are as in Fig. 4. The dotted line in the upper left panel is a straight line from the origin; the thin solid line is drawn with the same slope as the age-varying sequence in Fig. 9.

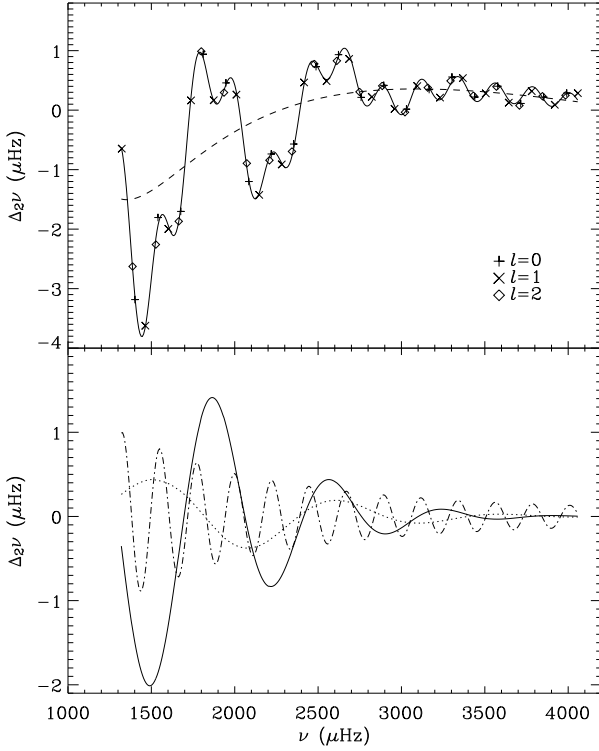


Figure 11. Top: The symbols are second differences $\Delta_2\nu$, defined by equation (2), of low-degree ($l=0,1,2$) eigenfrequencies obtained from adiabatic pulsation calculations of the central model 0, and have the same relation to l as in Fig. 1. The solid curve is the diagnostic D_2 determined by equations (21), (30) & (37), whose eleven parameters α_k have been adjusted to fit the data by least squares. The measure χ^2 (mean squared differences) of the overall misfit is $(53 \text{ nHz})^2$. The dashed curve represents the smooth contribution (last term in equation (21)). Bottom: Individual contributions of the oscillatory seismic diagnostic. The solid curve displays the He II contribution, the dotted curve is the He I contribution and the dot-dashed curve is the contribution from the base of the convection zone.

within the He I ionization zone (in the case of the Sun and similar stars, this is not the case of He II ionization), and the evanescence of the eigenfunction above the turning point must be taken into account. This can be achieved via the usual Airy-function representation. But for the purpose of evaluating the integral $\delta_\gamma \mathcal{K}$ it is adequate simply to use the appropriate high- $|\psi|$ sinusoidal or exponential asymptotic representations either side of the turning point to estimate the ‘oscillatory’ component of the integrand, which amounts to setting

$$[(\text{div}\xi)^2]_{\text{osc}} \simeq -\frac{\omega^3}{2\gamma p c r^2 \kappa} \cos 2\psi, \quad \text{for } \tau > \tau_t, \quad (34)$$

with ψ given by equation (27), without the subscripts II, and κ by equation (26). Despite the vanishing of κ at $\tau = \tau_t = (m+1)/\omega$, expression (34) is finite at $\tau = \tau_t$ because $2\psi(\tau_t) = \pi/2$. One can treat the evanescent region similarly, avoiding the singularity and making the representation continuous at $\tau = \tau_t$ by writing

$$[(\text{div}\xi)^2]_{\text{osc}} \simeq -\frac{\omega^3}{2\gamma p c r^2 |\kappa|} (1 - e^{2\psi - \pi/2}), \quad \text{for } \tau < \tau_t, \quad (35)$$

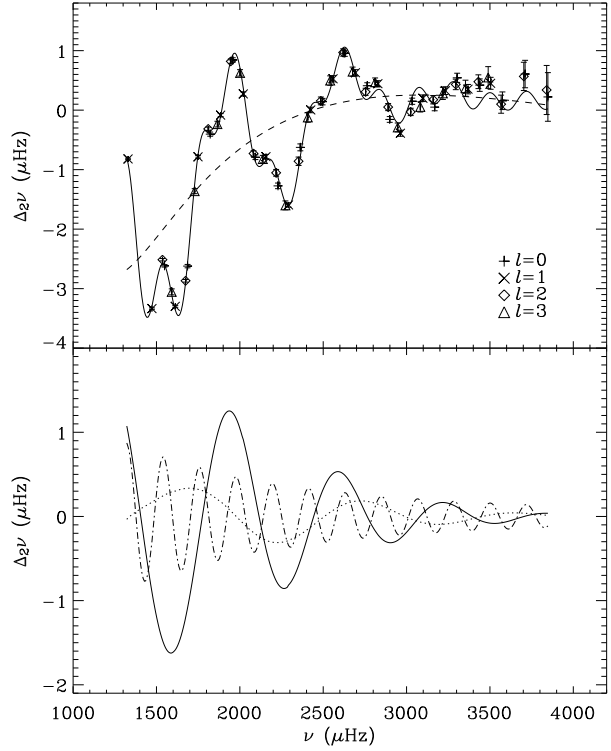


Figure 12. Top: The symbols (with error bars computed under the assumption that the raw frequency errors are independent) represent second differences $\Delta_2\nu$, defined by equation (2), of low-degree solar frequencies with $l=0,1,2$ and 3, obtained from BiSON (Basu et al. 2006). The effective overall error in the data is $\langle \sigma \rangle = 5.3 \text{ nHz}$. The solid curve is the diagnostic $D_2(\nu; \alpha_k)$, which has been fitted to the data in a manner intended to provide an optimal estimate of the eleven parameters α_k . The values of some of these fitting parameters are: $-\delta\gamma/\gamma|_{\tau_{\text{II}}} \simeq 0.047$, $\tau_{\text{II}} \simeq 819 \text{ s}$, $\Delta_{\text{II}} \simeq 70 \text{ s}$, and the measure E of the overall misfit is 33 nHz . The direct measure $\bar{\chi}$ is 2.1; the minimum- χ^2 fit of the function D_2 to the data yields $\bar{\chi}_{\text{min}} = 1.6$. The dashed curve represents the smooth contribution (last term in equation (21)). Bottom: Individual contributions of the seismic diagnostic. The solid curve displays the He II contribution, the dotted curve is the He I contribution and the dot-dashed curve is the contribution from the base of the convection zone.

where now

$$\psi(\tau) \simeq |\kappa|\tau\omega - (m+1) \ln \left(\frac{m+1}{\tau\omega} + |\kappa| \right) + \frac{\pi}{4}. \quad (36)$$

Although this expression has the wrong magnitude where $-\psi$ is large, that region makes very little contribution to the integral for $\delta_\gamma \mathcal{K}$. We have confirmed numerically that the formula (35) provides a tolerable approximation. At any point the integrand for $\delta_\gamma \mathcal{K}$ is the product of an exponential and a slowly varying function $\tilde{F}(\tau)$, say. Both $\tilde{F}(\tau)$ and $\psi(\tau)$ can be Taylor expanded about $\tau = \tilde{\tau}_1 = \tau_1 + \omega^{-1}\epsilon_1$ ($\epsilon_1 = \epsilon_{\text{II}}$) up to the quadratic term, rendering the approximation asymptotically integrable in closed form. The correction to the result of assuming $\tilde{F}(\tau) = \tilde{F}(\tilde{\tau}_1)$ and $\psi = \psi_1$ is small, so we actually adopt just the leading term.

The cyclic-eigenfrequency contribution to the entire helium glitch then becomes

$$\delta_\gamma \nu \simeq A_{\text{II}} \left[\nu + \frac{1}{2}(m+1)\nu_0 \right]$$

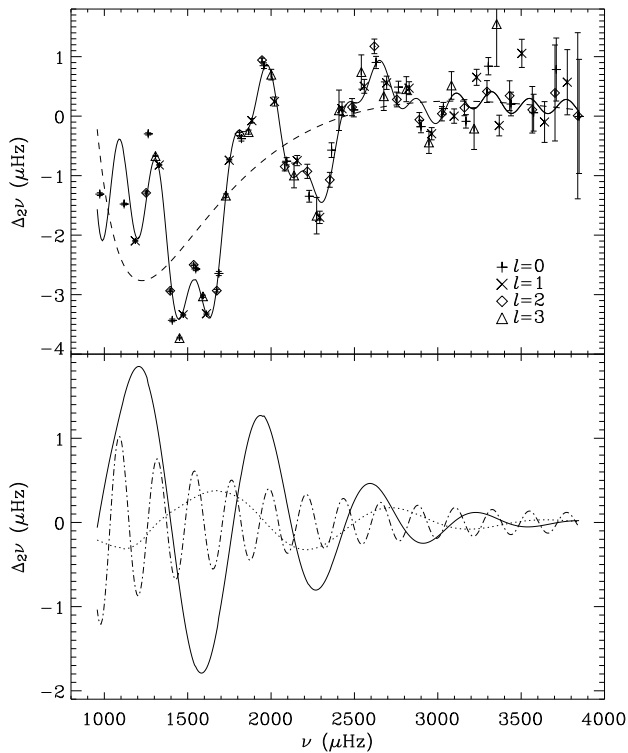


Figure 13. Similar to Fig. 12, but with the GOLF data that are plotted in Fig. 1. Top: The solid curve is the optimally fitted diagnostic $D_2(\nu; \alpha_k)$, with $-\delta\gamma/\gamma|_{\tau_{\text{II}}} \simeq 0.053$, $\tau_{\text{II}} \simeq 810$ s, and $\Delta_{\text{II}} \simeq 74$ s. The measure E of the misfit is 49 nHz, and $\bar{\chi} = 10.5$; the minimum- χ^2 fit of D_2 to the data yields $\bar{\chi}_{\text{min}} = 7.0$. The dashed curve is the smooth contribution. Bottom: Individual contributions to the seismic diagnostic, with the same notation as Fig. 12.

$$\times \left[\mu\beta\kappa_{\text{I}}^{-1} \left(e^{-8\pi^2\mu^2\kappa_{\text{I}}^2\Delta_{\text{I}}^2\nu^2} \cos 2\psi_{\text{I}} - 1 \right) + \kappa_{\text{II}}^{-1} \left(e^{-8\pi^2\kappa_{\text{II}}^2\Delta_{\text{II}}^2\nu^2} \cos 2\psi_{\text{II}} - 1 \right) \right], \quad (37)$$

provided $\tau_t < \tau_{\text{I}}$, in which κ_{II} is defined in Section 4.1 and κ_{I} is defined analogously; the phase ψ_{I} is given by $\psi_{\text{I}} = \psi(\tilde{\tau}_{\text{I}})$, where $\psi(\tilde{\tau}_{\text{I}})$ is given by equation (27), with $\tilde{\tau}_{\text{I}}$ replaced by $\eta\tilde{\tau}_{\text{II}}$, and with κ_{II} replaced by $\kappa_{\text{I}} = \kappa(\tilde{\tau}_{\text{I}})$. If $\tau_t > \tau_{\text{I}}$, we replace κ_{I} with $|\kappa_{\text{I}}|$ and $\cos 2\psi_{\text{I}}$ with $1 - \exp(2\psi_{\text{I}} - \pi/2)$, where now $\psi_{\text{I}} = \psi(\tilde{\tau}_{\text{I}})$ is given by equation (36).

Some of the parameters obtained by fitting to the numerical second differences the generalization $D_2(\nu; \alpha_k)$ of the asymptotic formula (22) obtained by using expression (37) for $\delta_\gamma\nu$, and still using equation (30) for $\delta_c\nu$, are plotted in Fig. 10. A comparison of the fitting parameters and of χ^2 between Figs 5, 6 and 10 shows that the improved seismic diagnostic D_2 results in an even better fit to the adiabatically computed eigenfrequencies than does the seismic diagnostic D_0 , which includes a description of only the He II ionization, and is also better than the seismic diagnostic D_1 with only the improved treatment of the asymptotic phase function.

A fit of the seismic diagnostic D_2 to $\Delta_2\nu$ of the adiabatically computed eigenfrequencies of the central stellar model 0 is shown in the top panel of Fig. 11, and a fit to $\Delta_2\nu$ of solar-frequency observations by BiSON (Basu et al. 2006)

in the top panel of Fig. 12. It demonstrates how well the oscillatory contributions to the second frequency differences of low-degree acoustic modes are approximated by our seismic diagnostic, at least for frequencies above $1300\mu\text{Hz}$. The lower panels in both figures show the individual contributions from He I He II and from the discontinuity in $d^2 \ln \rho/dr^2$ at the base of the convection zone.

It seems likely that because the ionization diagnostic, and also the signature of the base of the convection zone, are greatest at the lowest frequencies, it is important for our purpose that the frequencies of the gravest modes of the star be measured; indeed, those modes are the least influenced by the convective fluctuations near the stellar surface, and therefore their frequencies are in principle the most precisely defined, although they are apt to have low amplitudes and consequently be difficult to detect. We note that the GOLF data do extend to frequencies lower than the others, and with smaller standard errors. These modes dominate the fitting, as is evident from a comparison of the effective overall error $\langle \sigma \rangle$ of the modes in the entire GOLF data set and that of the subset within the MDI frequency range (see Section 2); the higher frequencies are relatively poorly determined. Consequently in the error-weighted fits illustrated in Figs 1 and 13, the gross properties of both the ionization signature and the signature of the base of the convection zone are determined predominantly by the lowest-frequency modes. However, we must emphasize that the asymptotic representation used to interpret the seismic diagnostic becomes less reliable at lower frequencies, and that therefore any model calibration might be more severely contaminated by structural properties other than that caused directly by He-induced ionization.

It would be unwise to attempt to infer Y directly from the values of the fitting parameters obtained from this investigation because the reference models were not computed with the most up-to-date microphysics; however, they are adequate for providing the partial derivatives needed for the calibration of a more realistic model.

One might wonder what the effect would be of including the degree dependence of the mode frequencies on the oscillatory component of $\delta\nu$. It can be taken into account by using the full leading-order asymptotic expression for the vertical component K of the wavenumber, which is given by equation (B2), and making the corresponding corrections to the eigenfunctions. For the purposes of estimating the numerators in equations (6) and (B9) it is adequate to ignore the buoyancy frequency and expand K just to leading order in l . More care must be taken in estimating the measures \mathcal{I} and \mathcal{I}_Ψ of the inertia, because the integrals extend down to the lower turning points of the modes where the degree-dependent term in K is as important as the other terms. The overall effect on $\delta_{\text{osc}}\nu$ is quite small, although, as we discuss in the next section, the l -dependence is not entirely negligible. Indeed, by including the degree-dependence in the fitting procedure it is possible to reduce χ^2 further, but only by about 10 per cent. The improvement, as can be seen in a plot analogous to Fig. 11, is noticeable only at low frequencies, for which the lower turning points are higher in the star and have a larger impact on the modes. However, the resulting modifications to the parameters $\delta\gamma/\gamma|_{\tau_{\text{II}}}$, τ_{II} , Δ_{II} and τ_c are tiny. Therefore we pursue this matter no further.

The results of this investigation indicate that the

asymptotic expression for $\Delta_2\nu$ can be calibrated against observation to obtain tolerable estimates of aspects of the effect on γ of helium ionization. They therefore augur the success of a future asteroseismic calibration.

5 DISCUSSION

Although we have decided to ignore the degree-dependence in our fitting, it is at least instructive to enquire how the degree l influences the ionization signature in the second differences. To this end we study a model in which we omit the effects of the base of the convection zone, accounting for contributions to the second frequency differences from only the ionization zones. Such conditions are represented by an adiabatically stratified stellar model satisfying the following equations:

$$\frac{dp}{dr} = -\frac{Gm\rho}{r^2}, \quad (38)$$

$$\frac{dm}{dr} = 4\pi r^2 \rho, \quad (39)$$

$$\frac{d\rho}{dr} = -\frac{Gm\rho^2}{\gamma pr^2}, \quad (40)$$

where m is the mass enclosed in the sphere of radius r (not to be confused with the polytropic index which it represents elsewhere in this paper). In constructing the model we adopted $\gamma = \gamma(\rho, p, Y, Z)$ obtained from the EFF equation of state (Eggleton, Faulkner & Flannery 1973). The usual regularity condition $m/r^2 \rightarrow 0$ as $r \rightarrow 0$ and the boundary condition $\rho = \rho_c$ were adopted at the centre, and the conditions $m = M, p = p_s$ were imposed at the surface $r = R$, where p_s is obtained from model S of Christensen-Dalsgaard et al. (1996). There results an eigenvalue problem for the eigenvalue ρ_c .

First, we concentrate on the smooth contributions to the second frequency differences. We represented them by a third-degree polynomial in Sections 2 and 4, as in the last term in equation (21). The symbols in the upper left panel of Fig. 14 show second differences $\Delta_2\nu$ of adiabatically computed eigenfrequencies for a helium-free adiabatically stratified reference model ($Y_{\text{ref}} = 0, Z = 0.02$). The dotted lines connect symbols of like degree l . They differ only at the lowest frequencies, and by a relatively small amount (values for $l = 4$ lie the furthest from a single curve, as expected, but modes of such high degree are not considered elsewhere in this paper). In the upper right panel are plotted the second differences $\Delta_2\delta\nu$ of the oscillatory component associated with helium ionization of a model in which the helium abundance Y is 0.25 ($Z = 0.02$). They were obtained from evaluating numerically the formulae (6)–(8) obtained from the variational principle, with $\delta\gamma = \gamma|_{Y=0.25} - \gamma|_{Y=0.0}$ and with the numerically computed eigenfunctions ξ (the depth-dependence of $\delta\gamma$, plotted as a function of acoustic depth τ , is illustrated in the lower right panel of Fig. 14), and are essentially independent of degree l . With the help of equation (5) the second frequency differences of the $Y = 0.25$ model can be obtained by taking the sum of $\Delta_2\nu$ of the $Y = 0$ model and $\Delta_2\delta\nu$. The result is depicted in the lower left panel of Fig. 14. Once again the values associated with $l = 0, 1, 2$ and 3 fall almost on a single curve. Therefore ignoring l is quite a good procedure, as is indeed evident

from the fit to the second differences of the frequencies of the solar model presented in Fig. 11. That fit is not perfect, however, and it may be that it could be improved by extracting the l -dependence from the smooth contribution using the asymptotic relation (20). The l -dependence of the oscillatory component is weaker; it arises principally from the l -dependence of the inertia \mathcal{I} .

On the whole, the amplitudes $\delta\gamma/\gamma|_{\tau_{\text{II}}}$ of the acoustic glitch inferred by fitting the asymptotically derived formulae to the frequency differences $\Delta_2\nu$ of the test models described in Section 3.1 agree reasonably well with the actual values in the model, especially when our preferred expression for the phase function is used. The amplitude increases with Y , as it should, even when the He ionization zones are represented by only a single Gaussian function (at least for the model sequence in which age varies). We notice in passing, however, that Monteiro & Thompson (2005) report that if the triangular approximation is made to the depression in γ , then the inferred amplitude varies in the wrong sense. The other parameters in our fitting are not reproduced so well as the amplitude. The estimated widths Δ_{II} are rather small, which is not what one would expect at least from Fig. 8, because the actual perturbation to γ appears to be somewhat broader than the Gaussian approximation used to represent it, although not by as much as the differences suggested by comparing Figs 9 and 10; it is comforting, however, that when the two helium ionizations are treated separately, as they should be, the magnitude of the discrepancy in Δ_{II} is the least. Also in error are the acoustic depths of the He II ionization zones and the bases of the convection zones, although they are better when the improved phase function is employed, as one would expect. We suspect that the remaining errors with the improved phase function have arisen because the actual models, and real stars too, are not polytropes: also there is some ambiguity in obtaining an appropriate location of the effective acoustic surface of the Sun, and hence the origin of the coordinate τ , because that depends on precisely how the layers in the convection zone near the upper turning points influence the dynamics of the modes, and consequently how the region adopted for the extrapolation of c^2 or ω_a^2 should be chosen; moreover, the deviation of the stratification from the polytropic behaviour influences the relation between ψ and our polytropic approximation throughout the convection zone, resulting in the errors in ψ_{II} and ψ_c being different. Finally, we note that the value of A_c inferred from the seismic calibration is 20% too low, which is puzzling because we would expect the asymptotic expressions used to relate the discontinuity in the second density derivative to the amplitude of the oscillatory signature to work rather well. Perhaps a significant source of the discrepancy is our neglect of the influence of the discontinuity in ω_a on the structure of the oscillation eigenfunctions (see Appendix B). In any case, we stress that the precision of the asteroseismic calibrations that are planned does not rely directly on the precision of the asymptotic expressions. Those expressions have been used solely to design seismic signatures of certain properties of the stratification of a star to be as free from contamination by other properties as can reasonably be expected; their role is to enable one to interpret the results of the calibrations, and to help in the assessment of the accuracy of the inferences.

It is noteworthy that the slopes of the solid and dashed

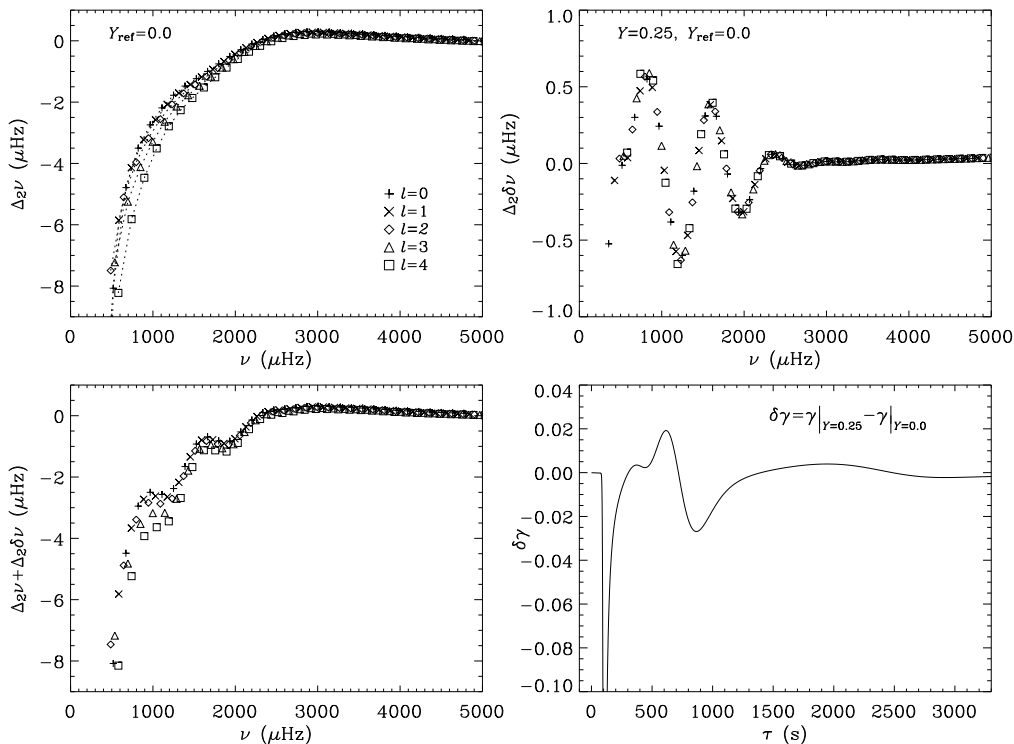


Figure 14. Calculated second frequency differences for adiabatically stratified models. The upper left panel shows the results for a reference model with helium-free gas ($Y_{\text{ref}} = 0.0$, $Z = 0.02$). The upper right panel shows the second differences of the frequency perturbation $\delta\nu$ according to equations (6)–(8) ($\delta\nu = \delta\omega/2\pi$) with $\delta\gamma = \gamma|_{Y=0.25} - \gamma|_{Y=0.0}$ being the difference in γ between the reference model computed with $Y_{\text{ref}} = 0.0$ and a model with $Y = 0.25$; $\delta\gamma$ is depicted in the lower right panel. The sum of $\Delta_2\nu$ and $\Delta_2\delta\nu$ is plotted in the lower left panel; it is an estimate of the second frequency differences of the $Y = 0.25$ model. The meanings of the symbols in the first three panels are indicated in the first panel. All results are obtained with the numerically computed eigenfunctions of the (unperturbed) reference model.

lines representing the behaviour of the two different sequences of solar models in the top three panels of Figs 4, 5, 6, 9 and 10 are not parallel. The variations of τ_{II} and Δ_{II} are both small, and can be influenced by details of the upper superadiabatic boundary layer in the convection zone, for example, which is not of principal concern here. But one might naively expect, and indeed hope, the values of $\delta\gamma/\gamma|_{\tau_{\text{II}}}$ to depend almost solely on the value of Y , for then the interpretation would have been simple. But that is evidently not the case. A substantial direct influence of heavy elements on the depression of γ by HeII ionization may be partially responsible. But it is likely that the predominant influence comes about through the dependence on the specific entropy s of the adiabat deep in the convection zone, which is determined by the (Z -dependent) calibration of the models to the solar radius and luminosity. We reiterate that nevertheless this result does not compromise the precision of the asteroseismic calibration, just its interpretation. It is no surprise that the slopes of $A_c(Y)$ and $\tau_c(Y)$ are different for the two sequences of solar models, because they depend on the interfacing of the convection zone with the radiative interior, and the latter is quite sensitive to the opacity, and hence to the value of Z (and, therefore in a calibrated sequence of solar models, to Y).

Our investigation has been carried out with a single equation of state. Although it can hardly be doubted that our signature of the magnitude of the depression in γ is quite

robust, it is certainly the case that relating that to Y is less so. The value of $\delta\gamma/\gamma|_{\tau_{\text{II}}}$ is determined locally by the values of Y and s , and the magnitude of the error in how they are related depends directly on the error in the equation of state at τ_{II} , although it is also due partly to the inaccuracy of our representation of the glitch (see Fig. 7). The error would certainly be adequately small for the asteroseismic calibrations of the foreseeable future. But to determine the value of Y does seem to require knowledge of s , which can be determined only by an additional diagnostic. That diagnostic might have been dependent on uncertainties in conditions far from the HeII ionization zone, which may be difficult to assess. But fortunately the immediate environment of the helium ionization zone is isentropic, so one needs to determine only a constant, rather than a function: given s (and the gravitational acceleration, which hardly varies through the helium ionization zones of solar-like stars, and to a high degree of precision may be considered to be constant too), the functional form of γ is rather well constrained, and a simply measurable property of it, such as Δ_{II} , might be used to obtain another, different, relation between Y and s . That would enable each of these two quantities to be determined. The constancy of s disengages the calibration from uncertainties elsewhere in the star. (We expect the value of τ_{II} to be less useful for these purposes, for it depends on conditions in the vicinity of the upper turning points of the modes; it should, however, be useful as a diagnostic of the treatment of

convection, which determines the structure of the superadiabatic boundary layers.) However, before such a calibration is carried out, more thorough tests of the reliability of the inferred value of Δ_{II} must be performed. Essentially the same suggestion has been made already by Monteiro & Thompson (2005) to distinguish between equations of state, although they too offered no cogent reason to suggest whether it would provide a reliable test. If the hypothesis that we are putting forward is correct, this measure of the specific entropy would not alone necessarily provide a robust criterion for selecting any particular equation of state. However, it would certainly limit the uncertainty in the $\delta\gamma$ - Y relation needed for the asteroseismic calibration.

We should also point out that the variation of γ in the He ionization zone would be influenced by the presence of a magnetic field, which we have ignored in this study. Evidence for low-amplitude solar-cycle variations has been seen in the raw frequencies of a combination of solar models of both low and intermediate degree (e.g. Goldreich et al. 1991), which relate directly to conditions in the He II ionization zone (Gough 1994), and, more recently, in fourth frequency differences (Basu & Mandel 2004, 2006). Such variations could be greater in other stars, and would therefore noticeably contaminate the low-degree diagnostic. Unless adequately accounted for, they would degrade any seismic calibration of Y .

We emphasize that our aim in this work is not to invent a functional representation of the second frequency differences, the diagnostic of our choice, or of any other diagnostic for that matter, with the intention of merely being able to fit the data well. Instead, it is principally to obtain a formula that can be related directly to properties of the stratification of the star that we believe to be pertinent to the abundance of helium. Although the degree to which we succeed in fitting the data provides some measure of our success, it is not the sole criterion guiding our choice of function. Indeed, functions that are not obviously directly related to the stratification but which are tailored to mimic the data should be almost bound to fit the data better. But evidently they must be less reliable for diagnosis. It is encouraging, however, that our function actually does fit the frequency data better than any other that has been tried before (Houdek & Gough 2006), particularly when the data are fitted over a large range of frequency, although we hasten to add that its ability to measure the acoustic glitches is not perfect. In this regard it is interesting to note that the fit to the GOLF data of D_2 , illustrated in Fig. 13, is no better than the fit of D_1 , illustrated in Fig. 1, yet the values inferred for $-\delta\gamma/\gamma|_{\tau_{\text{II}}}$, τ_{II} and Δ_{II} are likely to be superior.

Finally, we emphasize that although our analysis is based on asymptotic theory, the actual calibrations would be carried out using numerically computed eigenfrequencies, and their precision would be independent of the accuracy of the asymptotics. As is often the case in asteroseismology, the role of the asymptotics is to motivate the design of a calibration procedure, and to facilitate its interpretation in physical terms; it is not used in the calibration itself.

6 SUMMARY AND CONCLUSION

We have designed asteroseismic signatures of helium ionization which we trust will provide a reliable basis for calibrating stars against a suitable grid of theoretical models, using second frequency differences $\Delta_2\nu_{n,l} = \nu_{n-1,l} - 2\nu_{n,l} + \nu_{n+1,l}$. Those signatures can be used to determine the magnitudes, widths and locations of the depressions $\delta\gamma$ of the first adiabatic exponent γ due to He ionization.

The degree to which our original simple diagnostic (22) appears to reproduce the magnitude and width of the depression in γ in the He II ionization zone can be judged by comparing the inferred values plotted in Fig. 5 with those measured from the models in Fig. 4. The values of the amplitudes of the depression are overestimated by some 50%, and the widths underestimated by a similar amount, yielding an approximately correct magnitude of the glitch integral, Γ_{II} . However, the slopes of the dependence of those values on helium abundance Y , particularly amongst models with varying heavy-element abundance Z , are not reproduced. In this regard it should be appreciated that the reason may actually be that our procedure for characterizing the amplitudes and widths of the depressions in the models may not be seismically appropriate. The variation of the acoustic depth τ_{II} of the centre of ionization is more-or-less reproduced. However, the actual magnitude appears to be discrepant; that is due in part to our crude representation of acoustic phase, and perhaps in part to an uncertainty in the origin of τ . Roughly half of that discrepancy is accounted for by our improved treatment of the phase, discussed in Section 4.1, as can be seen in Fig. (6). That improvement also brings the amplitude of the γ depression almost into agreement with the model values, but the improvement in the inferred widths Δ_{II} is only slight. We suspected that the problem with the widths arises from our explicit neglect of He I ionization in our diagnostic formula, in which we represented the two distinct helium depressions, which in reality separately influence the oscillation eigenfrequencies, by a single Gaussian function. However, we note that the variation of Δ_{II} is less than the variation of the other ionization-related quantities, and may therefore perhaps not be a robust diagnostic. Nevertheless, we have introduced a separate representation of He I ionization in Section 4.2, the result of which can be assessed by comparing with model values in Fig. 9 with the seismically inferred counterparts plotted in Fig. 10. Interestingly, the slope with respect to Y of the measured model values of τ_{II} for the Z -varying sequence are changed, whereas that of the inferred values is not. Moreover, the slope of the amplitudes of the inferred γ depressions in the Z -varying sequence is improved only slightly. But the magnitude of the discrepancy between the inferred and the actual values of Δ_{II} is reduced by a factor three.

We have found that, for solar-like stars at least, the magnitude of $\delta\gamma$ increases approximately linearly with helium abundance Y , a property which has assisted us in accounting for the He I ionization zone by relating it directly to the contribution from He II ionization. By so doing, a somewhat more faithful overall representation of the He II ionization is achieved by the seismic calibration. The magnitude of the depression in γ is not a function of Y alone, but depends also on at least one more parameter. We argue that for a solar calibration there is just one, namely the specific

entropy; for other stars it must depend also on the gravitational acceleration, whose determination would be part of the overall calibration. If the situation is indeed that simple, then a potential asteroseismic calibration procedure is almost in hand.

ACKNOWLEDGEMENTS

We are very grateful to Jørgen Christensen-Dalsgaard for reading an earlier version of the paper and suggesting improvements, and to Philip Stark for enlightening correspondence. We thank Thierry Toutain and Sasha Kosovichev for supplying the MDI data, J. Ballot for supplying the GOLF data plotted in Figs 1 and 13, and Bill Chaplin for supplying the BiSON data plotted in Fig. 12. Support by the Particle Physics and Astronomy Research Council is gratefully acknowledged.

REFERENCES

- Ballot J., Turck-Chièze, S., García R.A., 2004, *A&A*, 423, 1051
- Balmforth N.J., Gough D.O., 1990, *ApJ*, 362, 256
- Baglin A., 2003, *Advances Space Res.*, 31, 345
- Basri G.B., Borucki W.J., Koch D.G., 2005, *New Astronomy Rev.*, 49, 478
- Basu S., 1997, *MNRAS*, 288, 572
- Basu S., Antia H.M., 1995, *MNRAS*, 276, 1402
- Basu S., Mandel A., 2004, *ApJ*, 617, 155
- Basu S., Mandel, 2006, in Lacoste H., ed., 10 years of SOHO and beyond. ESA SP-617, Noordwijk, in press.
- Basu S., Antia H.M., Narasimha D., 1994, *MNRAS*, 267, 209
- Basu S., Mazumdar A., Antia H. M., Demarque P., 2004, *MNRAS*, 350, 277
- Basu S., Chaplin W.J., Elsworth Y., New A.M., Serenelli G., Verner G.A., 2006, *ApJ*, submitted
- Baturin V.A., Mironova I.V., 1990a, *Sov. Astron. Lett.*, 16, 108
- Baturin V.A., Mironova I.V., 1990b, *Pisma Astron. Zh.*, 16, 253
- Borucki W.J., Koch D.G., Lissauer J.J., Basri G.B., Caldwell J.F., Cochran W.D., Dunham E.W., Geary J.C., Latham D.W., Gilliland R.L., Caldwell D.A., Jenkins J.M., Kondo Y., 2003, in Blades J.C., Siegmund H.W., eds, *Proceedings of the SPIE: Future EUV/UV and Visible Space Astrophysics Missions and Instrumentation*. Vol. 4854, p. 129
- Brodsky M.A., Vorontsov S.V., 1987, *Pisma Astron. Zh.*, 13, 438
- Chandrasekhar S., 1963, *ApJ*, 138, 896
- Christensen-Dalsgaard J., 1981, *MNRAS*, 194, 229
- Christensen-Dalsgaard J., 1986, in Gough D.O., ed., *Seismology of the Sun and distant Stars*. Nato ASI C169, Reidel, Dordrecht, p. 23
- Christensen-Dalsgaard J., Gough D.O., 1980, *Nat*, 288, 544
- Christensen-Dalsgaard J., Gough D.O., 1981, *A&A*, 194, 176
- Christensen-Dalsgaard J., Gough D.O., 1984, in Ulrich R.K., Harvey J., Rhodes Jr E.J., Toomre J., eds, *Solar Seismology from Space*. JPL Publ. 84-84, Pasadena, p. 199
- Christensen-Dalsgaard J., Pérez Hernández F., 1992, *MNRAS*, 257, 62
- Christensen-Dalsgaard J., Gough D.O., Thompson M.J., 1991, *ApJ*, 378, 413
- Christensen-Dalsgaard J., Duvall Jr T.L., Gough D.O., Harvey J.W., Rhodes Jr E.J., 1985, *Nat*, 315, 378
- Christensen-Dalsgaard J., et al., 1996, *Sci*, 272, 1286
- Cox A.N., Steward J.N., 1970a, *ApJS*, 19, 243
- Cox A.N., Steward J.N., 1970b, *ApJS*, 19, 261
- Däppen W., Gough D.O., Thompson M.J., 1988, in Rolfe E.J., ed., *Seismology of the Sun and Sun-like Stars*. ESA SP-286, Noordwijk, p. 505
- Däppen W., Gough D.O., Kosovichev A.G., Thompson M.J., 1991, in Gough D.O., Toomre J., eds, *Challenges to Theories of the Structure of Moderate-mass Stars*. Lecture Notes in Physics, Vol. 388, Springer Verlag, Heidelberg, p. 111
- Eggleton P., Faulkner J., Flannery B.P., 1973, *A&A*, 23, 325
- Goldreich P., Murray N., Willette G., Kumar P., 1991, *ApJ*, 370, 387
- Gough D.O., 1984a, *Mem. Soc. Astron. Ital.*, 55, 13
- Gough D.O., 1984b, *Phil. Trans. R. Soc. Lond.*, A, 313, 27
- Gough D.O., 1986a, in Gough D.O., ed., *Seismology of the Sun and distant Stars*. Nato ASI C169, Reidel, Dordrecht, p. 283
- Gough D.O., 1986b, in Osaki Y., ed., *Hydrodynamic and Magnetohydrodynamic Problems in the Sun and Stars*. University Tokyo Press, Tokyo, p. 117
- Gough D.O., 1987, *Nat*, 326, 257
- Gough D.O., 1990, in Osaki Y., Shibahashi H., eds, *Progress of Seismology of the Sun and Stars*. Lecture Notes in Physics, Vol. 367, Springer Verlag, Heidelberg, p. 283
- Gough D.O., 1993, in Zahn J.-P., Zinn-Justin J., eds, *Astrophysical fluid dynamics*. Amsterdam, Elsevier, p. 399
- Gough D.O., 1994, in Pap J.M., Fröhlich C., Hudson H.S., Solanki S.K., eds, *The Sun as a variable star*. Proc. IAU Colloq., 143, Cambridge University Press, Cambridge, p. 252
- Gough D.O., 1998, in Kjeldsen H., Bedding T., eds, *Proceedings of the First MONS Workshop*. Aarhus Universitet, Aarhus, p. 33
- Gough D.O., 2001, in von Hippel T., Simpson C., Manset N., eds., *ASP Conf. Ser. 245, Astrophysical Ages and Timescales*. Astron. Soc. Pac., San Francisco, p. 31
- Gough D.O., 2002, in Favata F., Roxburgh I.W., Galadi D., eds, *Stellar structure and habitable planet finding*. ESA SP-485, Noordwijk, p.65
- Gough D.O., Novotny E., 1990, *Solar Physics*, 128, 143
- Gough D.O., Vorontsov S.V., 1995, *MNRAS*, 273, 573
- Grevesse N., 1984, *Physica Scripta*, T8, 49
- Grundahl F., Kjeldsen H., Frandsen S., Andersen M., Bedding T., Arentoft T., Christensen-Dalsgaard J., 2006, *Mem. Soc. Astron. Ital.*, 77, 458
- Houdek G., Gough D.O., 2006, in Fletcher K., ed., *Proc. SOHO 18/GONG 2006/HelAs I, Beyond the Spherical Sun*. ESA SP-624, Noordwijk, in press
- Kjeldsen H., Bedding T.R., Butler R.P., Christensen-Dalsgaard J., Kiss L.L., McCarthy C., Marcy G.W., Tinney C.G., Wright J.T., 2005, *ApJ*, 635, 1281
- Kosovichev A.G., 1993, *MNRAS*, 265, 1053

- Kosovichev A.G., Christensen-Dalsgaard J., Däppen W., Dziembowski W.A., Gough D.O., Thompson M.J., 1992, MNRAS, 259, 536
- Lopez I., Gough D.O., 2001, MNRAS, 322, 472
- Lopez I., Turck-Chièze S., Michel E., Goupil M.-J., 1997, ApJ, 480, 794
- Lynden-Bell D., Ostriker, J., 1967, MNRAS, 136, 293
- Miglio A., Christensen-Dalsgaard J., Di Mauro M.P., Monteiro M.J.P.F.G., Thompson M.J., 2003, in Thompson M.J., Cunha M.S., Monteiro M.J.P.F.G., eds, Asteroseismology across the HR Diagram. Kluwer, Dordrecht, p. 537
- Monteiro M.J.P.F.G., Thompson M., 1998, in Deubner F.-L., Christensen-Dalsgaard J., Kurtz D., eds. Proc. IAU Symp. 185, New Eyes to see inside the Sun and Stars. Kluwer, Dordrecht, p. 317
- Monteiro M.J.P.F.G., Thompson M., 2005, MNRAS, 361, 1187
- Monteiro M.J.P.F.G., Christensen-Dalsgaard J., Thompson M., 1994, A&A, 283, 247
- Pérez Hernández F., Christensen-Dalsgaard J., 1994a, MNRAS, 267, 111
- Pérez Hernández F., Christensen-Dalsgaard J., 1994b, MNRAS, 269, 475
- Pérez Hernández F., Christensen-Dalsgaard J., 1998, MNRAS, 295, 344
- Piau L., Ballot J., Turck-Chièze S., 2005, A&A, 430, 571
- Roxburgh I.W., Vorontsov S.V., 1994, MNRAS, 268, 880
- Shibahashi H., Noels A., Gabriel M., 1983, A&A, 123, 283
- Tassoul M., 1980, ApJS, 43, 469
- Ulrich R.K., 1986, ApJ, 306, L37
- Ulrich R.K., Rhodes Jr E.J., 1983, ApJ, 265, 551
- Verner G.A., Chaplin W.J., Elsworth Y., 2004, MNRAS, 351, 311
- Vorontsov S.V., 1988, in Rolfe E.J., ed., Seismology of the Sun and Sun-like Stars. ESA SP-286, Noordwijk, p. 475
- Vorontsov S.V., Baturin V.A., Pamyatnykh A.A., 1991, Nat, 349, 49
- Vorontsov S.V., Baturin V.A., Pamyatnykh A.A., 1992, MNRAS, 257, 32

APPENDIX A: SIGNATURE OF RAPID VARIATION OF THE ADIABATIC EXPONENT

The adiabatic eigenfrequencies ω of a nonrotating star in the Cowling approximation satisfy a variational principle which can be written in the form (Chandrasekhar 1963)

$$\omega^2 = \frac{\mathcal{K}}{\mathcal{I}} \quad (\text{A1})$$

where

$$\mathcal{K} = \frac{1}{4\pi} \int [\gamma p (\text{div} \boldsymbol{\xi})^2 + 2(\boldsymbol{\xi} \cdot \nabla p) \text{div} \boldsymbol{\xi} + (\boldsymbol{\xi} \cdot \nabla p)(\boldsymbol{\xi} \cdot \nabla \ln \rho)] dV \quad (\text{A2})$$

and

$$\mathcal{I} = \frac{1}{4\pi} \int \rho \boldsymbol{\xi} \cdot \boldsymbol{\xi} dV, \quad (\text{A3})$$

the integrals being over the volume of the star. Omitted from equation (A1) is a possible surface integral; that integral contributes to ω at most a slowly varying function (with respect to ω), which in any case in practice is small, so we have ignored it at the outset for simplicity. By adopting the

Cowling approximation we have also ignored the contribution from the gravitational-potential perturbation, because that too is only slowly varying. For low-degree modes of high order, the integrand in \mathcal{K} is dominated by the first term (whose integral we call \mathcal{K}_1), except possibly in localized regions where the equilibrium density ρ varies abruptly, such as at the base of the convection zone. Therefore the contribution to $\delta\omega$ from a region of relatively rapid variation of γ produced by the ionization of an abundant element may be approximated by

$$\delta\omega \simeq \frac{\delta\mathcal{K}_1 - \omega^2 \delta\mathcal{I}}{2\omega\mathcal{I}} \simeq \frac{\delta\mathcal{K}_1}{2\omega\mathcal{I}}, \quad (\text{A4})$$

since $|\delta\mathcal{K}_1| \gg \omega^2 |\delta\mathcal{I}|$, where

$$\delta\mathcal{K}_1 = \frac{1}{4\pi} \int (\delta\gamma) p (\text{div} \boldsymbol{\xi})^2 dV + \frac{1}{4\pi} \int \gamma (\delta p) (\text{div} \boldsymbol{\xi})^2 dV \quad (\text{A5})$$

$$=: \delta_\gamma \mathcal{K}_1 + \delta_p \mathcal{K}_1 \quad (\text{A6})$$

and

$$\delta\mathcal{I} = \frac{1}{4\pi} \int \delta\rho \boldsymbol{\xi} \cdot \boldsymbol{\xi} dV, \quad (\text{A7})$$

in which $\delta\gamma$ and δp are to be regarded as the differences between γ and p in the equilibrium star and those in a similar smooth model in which ionization is absent. In view of the variational principle, the differences (presumed to be small) between the values of $\boldsymbol{\xi}$ in the star and in the smooth model do not contribute to $\delta\omega$ to leading order in small quantities. If $\delta\gamma$ is defined to be nonvanishing only in the ionization region where it varies rapidly with r , then one expects $\delta_\gamma \mathcal{K}_1$ to contribute the dominant oscillatory (with respect to frequency) component to ω , because δp , which is related to $\delta\gamma$ via its radial derivative, varies with r more slowly, as does $\delta\rho$ which in the helium ionization zone is directly related to δp through the adiabatic constraint. (Note that for low-amplitude perturbations δp , $\delta\rho$, $\delta\gamma$, the relation between $\delta\rho$ and δp does not depend on $\delta\gamma$ to leading order.) We have confirmed numerically that this is indeed the case. Consequently, most of the oscillatory contribution to $\delta\omega$, in the absence of rotation, is contained in the term $(2\omega\mathcal{I})^{-1} \delta_\gamma \mathcal{K}_1$.

In estimating the integrals \mathcal{I} and \mathcal{K} it is adequate for our purposes to use the high-order, low-degree asymptotic expressions for the eigenfunctions of the smooth model, and then to evaluate the integrals asymptotically. In solar-like stars the He II ionization zone is well inside the propagating region of the acoustic modes, and the leading term in the Liouville-Green approximation to the solution of the adiabatic wave equation suffices, as is described in Section 2. That is not necessarily the case for the He I ionization zone, and formally one should retain the Airy-function form of the JWKB approximation. However, for the purpose of evaluating \mathcal{K} , we have found it sufficient to adopt the large-phase sinusoidal or exponential representations either side of the upper turning point τ_t of the mode, even up to the turning point itself, but scaling the eigenfunction $\text{div} \boldsymbol{\xi}$ in the evanescent zone with a constant chosen to render that eigenfunction continuous at $r = r_t$.

Rotation influences the eigenfrequencies via the Coriolis force (with respect to a rigid frame of reference rotating locally with the fluid) and via centrifugal effects which both influence the oscillation dynamics directly and distort the equilibrium structure of the star from sphericity. One can

estimate the influence with an analysis similar to that presented here using the more general variational principle of Lynden-Bell & Ostriker (1967). In particular, one would obtain an estimate of the oscillatory contribution to modes of like degree l and azimuthal order m induced by a tachocline flow near the base of the convection zone of an essentially axisymmetric star. However, if ω is regarded as the multiplet frequency, obtained as the equally weighted average of the frequencies of all the modes of like l and n , but varying azimuthal order, such contributions are suppressed, at least when rotation is slow (e.g. Gough 1993). Then the multiplet frequencies provide a good diagnostic of helium ionization. However, if the centrifugal force is not negligible, its average effect on the equilibrium structure of the star would need to be taken into account in the grid of reference stellar models used for comparison.

APPENDIX B: SIGNATURE OF THE ACOUSTIC GLITCH AT THE BASE OF THE CONVECTION ZONE

The acoustic glitch at the base of the convection zone is essentially a discontinuity in the second derivative of the temperature, associated with which are discontinuities in the second derivatives of sound speed and density. That renders all three terms in the integrand for \mathcal{K} , given by equation (A2), susceptible to perturbations of the same order. Then terms must be calculated with some care, because there can be cancellation in leading order when the terms are combined (e.g. Monteiro, Christensen-Dalsgaard & Thompson 1994). It is more straightforward, however, to work directly (in the planar Cowling approximation) with the single second-order differential equation for the r -dependent factor $\tilde{p}(r)$ in the Lagrangian pressure perturbation eigenfunction, for then only one quantity is discontinuous, namely the acoustic cutoff frequency ω_a (and, of course, the second derivative of the eigenfunction). That equation is (e.g. Gough 1993)

$$\frac{d^2\Psi}{dr^2} + K^2\Psi = 0, \quad (\text{B1})$$

where $\Psi \sim r\rho^{-1/2}\tilde{p}$. The vertical wavenumber is given by

$$K^2 = \frac{\omega^2 - \omega_a^2}{c^2} - \frac{l(l+1)}{r^2} \left(1 - \frac{N^2}{\omega^2}\right), \quad (\text{B2})$$

in which N is the buoyancy (Brunt-Väisälä) frequency:

$$N^2 = g \left(\frac{1}{H} - \frac{g}{c^2} \right); \quad (\text{B3})$$

also

$$\omega_a^2 = \frac{c^2}{4H^2} \left(1 - 2\frac{dH}{dr}\right) = \frac{c^2}{4H^2} - \frac{c^2}{2} \frac{d^2 \ln \rho}{dr^2}, \quad (\text{B4})$$

where g is the local acceleration due to gravity and $H = -(d \ln \rho / dr)^{-1}$ is the density scale height.

Equation (B1) is to be solved subject to a regularity condition at $r = 0$ and an appropriate causality condition at $r = R$. It is written in self-adjoint form, and therefore it follows immediately that for modes with frequencies well below the acoustic cutoff frequency characteristic of the at-

mosphere, the equation

$$\int_0^R \left(\frac{d\Psi}{dr} \right)^2 dr - \frac{l(l+1)}{\omega^2} \int_0^R \frac{N^2 \Psi^2}{r^2} dr + \int_0^R \left[\frac{\omega_a^2}{c^2} + \frac{l(l+1)}{r^2} \right] \Psi^2 dr - \omega^2 \int_0^R \frac{\Psi^2}{c^2} dr = 0 \quad (\text{B5})$$

defines a variational principle for ω^2 amongst acceptable functions Ψ ; those functions are such that the boundary terms that arise from the integration by parts to obtain the first term in equation (B5) either vanish (at $r = 0$) or can be neglected (at $r = R$) because they contribute at most a slowly varying function of ω . At the base of the convection zone, $r = r_c$, ω_a^2 suffers a discontinuity

$$\Delta_c \equiv [\omega_a^2]_{r_c^-}^{r_c^+}. \quad (\text{B6})$$

Let ω_a^2 be extrapolated smoothly from the convection zone down into the radiative interior to define ω_{as}^2 with the property $\omega_{as}^2 \rightarrow \omega_a^2$ as $r \rightarrow 0$. Additionally, let us define

$$\delta\omega_a^2 = \omega_a^2 - \omega_{as}^2, \quad (\text{B7})$$

which satisfies $\delta\omega_a^2 = 0$ for $r > r_c$, $\delta\omega_a^2 = -\Delta_c$ at $r = r_c$, and $\delta\omega_a^2 \rightarrow 0$ as $r \rightarrow 0$. Granted that $\delta\omega_a^2$ is small enough for linearization to be valid, the contribution $\delta_c\omega^2$ to $\delta\omega^2$ from the discontinuity in ω_a^2 is then given by

$$\delta_c\omega^2 \int_0^R \frac{\Psi^2}{c^2} dr + \frac{l(l+1)}{\omega^2} \int_0^R \frac{\delta N^2}{r^2} \Psi^2 dr - \frac{l(l+1)\delta_c\omega^2}{\omega^4} \int_0^R \frac{N^2}{r^2} \Psi^2 dr - \int_0^{r_c} \frac{\delta\omega_a^2}{c^2} \Psi^2 dr \simeq 0. \quad (\text{B8})$$

Formally it was necessary to include the second and third terms on the left-hand side of this equation because the variational principle holds only for perturbations in the model that preserve hydrostatic support, and changing ω_a^2 leads to a change δN^2 in N^2 . However, these terms are small for low-degree high-order p modes (and zero for radial modes). Consequently they can safely be ignored, yielding

$$\delta_c\omega^2 \simeq \frac{\int_0^{r_c} \delta\omega_a^2 c^{-2} \Psi^2 dr}{\int_0^R c^{-2} \Psi^2 dr} \equiv \frac{\delta_c \mathcal{K}}{\mathcal{I}_\Psi}. \quad (\text{B9})$$

This formula is adequate for the purposes of studying the signature of helium ionization. We note, however, that the linearization may not be adequate for studying the base of the convection zone; for that endeavour one may need to account for the perturbations to the eigenfunctions, as did Roxburgh and Vorontsov (1994). From asymptotic theory the high-order eigenfunctions can be approximated by (e.g. Gough 1993):

$$\Psi \sim \Psi_0 K^{-1/2} \sin \psi, \quad (\text{B10})$$

between the turning points r_b and r_t at which \mathcal{K} vanishes, where

$$\psi = \int_r^{r_t} K dr + \frac{\pi}{4}; \quad (\text{B11})$$

then

$$\begin{aligned} \mathcal{I}_\Psi &\simeq \int_{r_b}^{r_t} \Psi_0^2 c^{-2} K^{-1} \sin^2 \psi dr \\ &\simeq \frac{1}{2} \Psi_0^2 \int_{r_b}^{r_t} (cK)^{-1} \frac{dr}{c} \\ &\simeq \frac{1}{2\omega} \Psi_0^2 \int_{\tau_t}^{\tau_b} \left(1 - \frac{\omega_a^2}{\omega^2}\right)^{-1/2} d\tau \end{aligned}$$

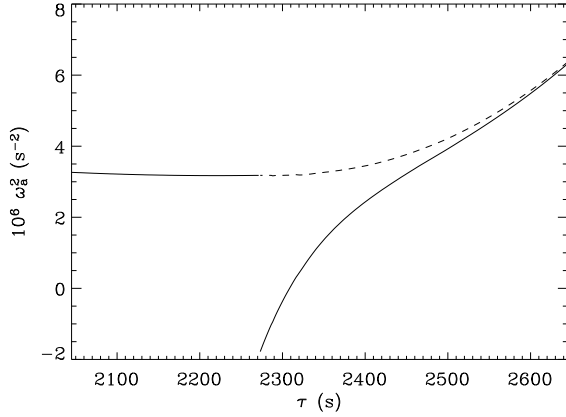


Figure B1. Acoustic cutoff frequency ω_a in the vicinity of the base of the convection zone. The solid curves show ω_a^2 of the central model 0 and the dashed curve is the sum of the solid curve and of equation (B15) evaluated with $\tau_0 = 80$ s.

$$\simeq \frac{1}{2\omega} T \Psi_0^2, \quad (\text{B12})$$

in which $\tau_t = \tau(r_t)$ and $\tau_b = \tau(r_b)$ are the acoustic depths of the upper and lower turning points. In our introductory analysis in Section 2 we ignored ω_a ; in that case the last of equations B12 follows immediately from the equation above. When ω_a is included in the polytropic approximation, as in Section 4.1, the first-order correction to \mathcal{I}_Ψ vanishes, and therefore equation (B12) still holds. We have also ignored the l -dependence of K , in the penultimate approximation in equations (B12), consistently with our reduction of equation (B8) to equation (B9). At this level of approximation, \mathcal{I}_Ψ becomes the same as the leading-order approximation (13) to the inertia \mathcal{I} defined by equation (8) after setting $\Psi_0 = \omega$.

The integral $\delta_c \mathcal{K}$ in equation (B9) can be approximated by

$$\begin{aligned} \delta_c \mathcal{K} &\simeq \Psi_0^2 \int_{r_b}^{r_c} \delta \omega_a^2 c^{-2} K^{-1} \sin^2 \psi \, dr \\ &\simeq \frac{1}{2} \Psi_0^2 \int_{r_b}^{r_c} \delta \omega_a^2 (cK)^{-2} [1 - \cos 2\psi] K \, dr. \end{aligned} \quad (\text{B13})$$

Once again it is adequate to set $K \simeq \omega/c$, and to set $\psi = \psi_c + \omega(\tau - \tau_c)$ with

$$\psi_c = \int_{r_c}^{r_t} K \, dr + \frac{\pi}{4}. \quad (\text{B14})$$

Furthermore, beneath the convection zone we approximate ω_a^2 by an exponential function:

$$\delta \omega_a^2 \simeq -\Delta_c e^{-(\tau - \tau_c)/\tau_0}, \quad (\text{B15})$$

where $\tau_0 \ll T$ is determined by fitting expression (B15) to the central model of our grid; it is compared with the model in Fig. B1. Then, since $\delta \omega_a^2$ varies much more rapidly than $(cK)^{-2}$ – in fact $cK \simeq \omega = \text{constant}$ – one may ignore the variation of the latter over a few τ_0 . It follows that the oscillatory component of $\delta_c \mathcal{K}$ is then

$$\begin{aligned} \delta_{c,\text{osc}} \mathcal{K} &\simeq \frac{1}{2} \omega \Delta_c \Psi_0^2 (cK)^{-2} \Big|_{r_c} \int_{\tau_c}^T e^{-(\tau - \tau_c)/\tau_0} \cos 2\psi \, d\tau \quad (\text{B16}) \\ &= \frac{1}{4} \Psi_0^2 (cK)^{-2} \Big|_{r_c} \left(1 + \frac{1}{4\tau_0^2 \omega^2}\right)^{-1/2} \Delta_c \end{aligned}$$

$$\times \cos [2\psi_c + \tan^{-1}(2\tau_0\omega)]. \quad (\text{B17})$$

Finally, we notice that only the second term in equation (B4) is discontinuous, whence

$$\Delta_c = -\frac{c^2}{2} \left[\frac{d^2 \ln \rho}{dr^2} \right]_{r_c^-}^{r_c^+}. \quad (\text{B18})$$

Setting $(cK)^2 \simeq \omega^2$ at the base of the convection zone, we finally obtain for the oscillatory contribution $\delta_{c,\text{osc}} \omega$ to ω from the discontinuity in the acoustic cutoff frequency at $r = r_c$:

$$\begin{aligned} \delta_{c,\text{osc}} \omega &\simeq \frac{c_c^2}{8T\omega^2} \left(1 + \frac{1}{4\tau_0^2 \omega^2}\right)^{-1/2} \left[\frac{d^2 \ln \rho}{dr^2} \right]_{r_c^-}^{r_c^+} \\ &\times \cos [2\psi_c + \tan^{-1}(2\tau_0\omega)], \end{aligned} \quad (\text{B19})$$

where $c_c = c(r_c)$.

Within our initial approximation discussed in Section 2, in which the acoustic cutoff frequency ω_a was not explicitly taken into account, we set $\psi_c = \tau_c \omega + \epsilon_c$, where ϵ_c is constant, as in equation (17). When ω_a is taken into account as in Section 4, the phase is $\psi_c = \psi(\tilde{r}_c)$, in which $\psi(\tilde{r}_c)$ is essentially given by equation (27) with \tilde{r}_{II} replaced by $\tilde{r}_c = \tau_c + \omega^{-1} \epsilon_c$:

$$\psi_c \simeq \kappa_c \tilde{r}_c \omega - (m+1) \cos^{-1} \left(\frac{m+1}{\tilde{r}_c \omega} \right) + \frac{\pi}{4}, \quad (\text{B20})$$

where $\kappa_c = [1 - (m+1)^2/\tilde{r}_c^2 \omega^2]^{1/2}$, which is tantamount to adding a frequency-dependent phase term to the constant ϵ_c . For stars with acoustically deep convection zones, the correction to the initial approximation is small, and the frequency dependence is therefore weak. In the case of the sun, for example, $\tilde{r}_c \omega \simeq 40$ for a 3 mHz mode, whence $d\psi_c/d\omega = \kappa_c \tilde{r}_c \simeq 0.995 \tilde{r}_c$.

APPENDIX C: SECOND DIFFERENCE OF THE OSCILLATORY FREQUENCY COMPONENT

Consider an oscillatory signal of the form

$$\delta \nu_n = A_n \cos x_n \quad (\text{C1})$$

with $\nu_n = \omega_n/2\pi$, where $A_n = A_n(\omega_n)$ and where $x_n = x_n(\omega_n)$ varies almost linearly with ω_n throughout the range of frequencies ω_n that we are considering. For clarity we have suppressed the index l . To estimate the second frequency difference $\Delta_2 \delta \nu_n \equiv \delta \nu_{n+1} - 2\delta \nu_n + \delta \nu_{n-1}$ we regard ω_n as a continuous function of n and expand $x_{n\pm 1}$ and $A_{n\pm 1}$ in Taylor series about x_n and A_n respectively, retaining only two terms for $x_{n\pm 1}$ and three for $A_{n\pm 1}$:

$$x_{n\pm 1} \simeq x_n \pm \alpha, \quad A_{n\pm 1} \simeq (1 \pm a + b) A_n, \quad n \gg 1, \quad (\text{C2})$$

where $\omega_0 = 2\pi\nu_0$ approximates the large (angular) frequency separation and

$$\alpha = \frac{d\omega_n}{dn} \frac{dx_n}{d\omega_n} \simeq \omega_0 \frac{dx_n}{d\omega_n}, \quad (\text{C3})$$

$$\begin{aligned} a &= \frac{1}{A_n} \frac{dA_n}{dn} \simeq \omega_0 \frac{d \ln A_n}{d\omega_n}, \\ b &= \frac{1}{2A_n} \frac{d^2 A_n}{dn^2} = \frac{1}{2A_n} \left[\left(\frac{d\omega_n}{dn} \right)^2 \frac{d^2 A_n}{d\omega_n^2} + \frac{d^2 \omega_n}{dn^2} \frac{dA_n}{d\omega_n} \right] \end{aligned}$$

$$\simeq \frac{\omega_0^2}{2A_n} \frac{d^2 A_n}{d\omega_n^2}. \quad (\text{C4})$$

The derivatives of ω_n are obtained by differentiating equation (20) with respect to n at fixed l ; it is consistent with the rest of this analysis to retain only the leading term: $d\omega_n/dn \simeq \omega_0$, $d^2\omega_n/dn^2 \simeq 0$. Substituting equations (C2) into the definition of the second difference yields

$$\begin{aligned} \Delta_2\delta\nu_n &= [(1+a+b)\cos(x_n+\alpha) - 2\cos x_n \\ &\quad + (1-a+b)\cos(x_n-\alpha)]A_n \\ &= FA_n \cos(x_n - \delta), \end{aligned} \quad (\text{C5})$$

where

$$F = 2\{[1 - (1+b)\cos\alpha]^2 + a^2 \sin^2\alpha\}^{1/2} \quad (\text{C6})$$

and

$$\delta = \tan^{-1} \left[\frac{a \sin \alpha}{1 - (1+b)\cos\alpha} \right]. \quad (\text{C7})$$

Had the frequency separation $\Delta_1\nu_n$ been small compared with the scale of variation on A_n , then $\Delta_1\delta\nu_n$ and $\Delta_2\delta\nu_n$ would approximate the first and second derivatives of $\delta\nu_n$ with respect to n ; but it is not, and the formulae (C5)–(C7) differ substantially from the second derivative.

In the first approximation to the contribution from HeII ionization given by equation (15), $A_n \propto \omega_n e^{-2\Delta_{\text{II}}^2\omega_n^2}$ and $x_n = 2(\tau_{\text{II}}\omega_n + \epsilon_{\text{II}})$. Therefore,

$$\alpha \simeq 2\omega_0\tau_{\text{II}}, \quad (\text{C8})$$

and

$$\begin{aligned} a &\simeq -(4\Delta_{\text{II}}^2\omega_n^2 - 1)\omega_0\omega_n^{-1}, \\ b &\simeq 2\Delta_{\text{II}}^2\omega_0^2(4\Delta_{\text{II}}^2\omega_n^2 - 3). \end{aligned} \quad (\text{C9})$$

In the case of the Sun, $\omega_0 \simeq 8.8 \times 10^{-4} \text{s}^{-1}$, $\Delta_{\text{II}} \simeq 80 \text{s}$ and $\tau_{\text{II}} \simeq 800 \text{s}$; whence $\alpha \simeq 1.4$. In the middle of the frequency range used for our calibration of solar models, $\omega_n \simeq 2\pi \times 2.7 \text{mHz} \simeq 1.7 \times 10^{-2} \text{s}^{-1}$; whence $a \simeq -0.33$ and $b \simeq 0.04$. The latter is so small partly because of a near cancellation of the two terms in parentheses at this frequency (cancellation is exact at $\nu \simeq 2 \text{mHz}$), but it never exceeds this value by more than a factor four in the frequency range of interest, and is greatest at the highest frequency where the amplitude A_n is the smallest. The effect of the neglected higher-order terms in the Taylor expansions of A_n and x_n is even smaller. The value of the amplitude factor $F \simeq 1.7$, and $\delta \simeq -0.4$.

When the acoustic cutoff and the second-order term in the asymptotic eigenfrequency relation (20) are taken into account, as in Section 4.1, the amplitude factor for the ionization glitch becomes $A_n \propto A_{\text{II}}\kappa_{\text{II}}^{-1}[\omega_n + (m+1)\omega_0/2] \exp(-2\kappa_{\text{II}}^2\Delta_{\text{II}}^2\omega_n^2)$ and $x_n = 2\psi_{\text{II}}$, where $\psi_{\text{II}} = \psi(\tilde{\tau}_{\text{II}})$, with $\tilde{\tau}_{\text{II}} = \tau_{\text{II}} + \omega^{-1}\epsilon_{\text{II}}$ and $\psi(\tilde{\tau}_{\text{II}})$ given by equation (27). Then

$$\alpha \simeq 2\omega_0\tilde{\tau}_{\text{II}}\kappa_{\text{II}}; \quad (\text{C10})$$

$\kappa_{\text{II}} = \kappa(\tilde{\tau}_{\text{II}})$ is given by equation (26), and

$$\begin{aligned} a &\simeq -[4\Delta_{\text{II}}^2\omega_n^2 + \kappa_{\text{II}}^{-2} - 1 - (1+\beta_a)^{-1}]\omega_0\omega_n^{-1}, \\ b &\simeq 2\Delta_{\text{II}}^2\omega_0^2[4\Delta_{\text{II}}^2\omega_n^2 - 1 - 2(1+\beta_a)^{-1}], \end{aligned} \quad (\text{C11})$$

where $\beta_a = \frac{1}{2}(m+1)\omega_0\omega_n^{-1}$. We have simplified the expression for b by ignoring a term $(m+1)^2/4\Delta_{\text{II}}^2\tilde{\tau}_{\text{II}}^2\omega_n^4$, and other yet smaller terms, which typically augment the already small b by only about 1 per cent. For the HeI contribution, one must replace κ_{II} and Δ_{II} by κ_{I} and Δ_{I} when

Table C1. Relative signal error magnification due to order- k differencing of frequencies, evaluated at $\nu=1.5, 2.75$ and 4.0mHz .

k	e_k/F_k					
	He II ionization zone			Base of convection zone		
	$\nu=1.5$	2.75	4.0 mHz	$\nu=1.5$	2.75	4.0 mHz
1	1.38	1.30	1.33	0.83	0.81	0.80
2	1.91	1.46	1.30	0.71	0.73	0.74
3	3.22	2.44	2.33	0.76	0.77	0.76
4	4.74	2.90	2.27	0.70	0.75	0.76
5	7.98	4.92	3.90	0.79	0.81	0.81
6	12.10	5.79	3.65	0.74	0.81	0.83
8	31.43	11.19	5.57	0.81	0.90	0.93
10	51.36	21.95	9.27	0.89	1.02	1.05

$\tau_t < \tau_1$. When τ_1 is in the evanescent zone of the mode, so that $\delta\nu_n = A_n \exp(-x_n)$, then $\Delta_2\delta\nu_n = FA_n \exp(-x_n)$, where $F = 2[(1+b)\cosh\alpha - 1 - a\sinh\alpha]$. The derivatives a and b are still given by equations (C10) and (C11), but now $\alpha \simeq 2\omega_0\tilde{\tau}_1|\kappa_1|$.

At the base of the convection zone, $x_n = 2\psi_c + \tan^{-1}(2\tau_0\omega_n) \simeq 2\psi_c$ and $\alpha \simeq 2\omega_0\tau_c$ because $\kappa_c = \kappa(\tilde{\tau}_c)$ is very close to unity. Here, $\tilde{\tau}_c = \tau_c + \omega^{-1}\epsilon_c$. Moreover, $A_n \propto \omega_n^{-2}(1 + 1/4\tau_0^2\omega_n^2)^{-1/2}$, whence

$$\begin{aligned} a &\simeq -2\omega_0\omega_n^{-1}(1 + 1/8\tau_0^2\omega_n^2)/(1 + 1/4\tau_0^2\omega_n^2), \\ b &\simeq \omega_0^2\omega_n^{-2}(3 + 5/8\tau_0^2\omega_n^2)/(1 + 1/4\tau_0^2\omega_n^2)^2. \end{aligned} \quad (\text{C12})$$

Again we have simplified b , this time by ignoring $1/48\tau_0^4\omega_n^4$ in the parentheses in the numerator, which typically contributes about 0.2 per cent. In the case of the Sun, $\tau_0 \simeq 80 \text{s}$ and $\tau_c \simeq 2273 \text{s}$ (see Fig. B1). Whence $a \simeq -0.10$ and $b \simeq 0.01$ in the middle of the frequency range, and $F \simeq 3.4$ and $\delta \simeq 0.05$.

It is interesting to estimate the signal-to-noise ratio for differences $\Delta_k\delta\nu_n$ of various orders k . It is straightforward to extend the analysis above to obtain formula of the kind: $\Delta_k\delta\nu_n = F_k A_n \cos(x_n - \delta_k)$. The frequency differences involve a weighted sum of $k+1$ frequency increments $\delta\nu_n$, which may be written

$$\Delta_k\delta\nu_n = \sum_{l=-k/2}^{k/2} d_{kl}\delta\nu_{n+l}, \quad (\text{C13})$$

where, for example, $d_{2l} = (1, -2, 1)$ and $d_{4l} = (1, -4, 6, -4, 1)$. Presuming, for simplicity, that the statistical uncertainties in the frequency measurements are independent, all with standard deviation σ , then the variance of the possible error in $\Delta_k\delta\nu_n$ is $e_k^2\sigma^2 = \sum_l d_{kl}^2\sigma^2$. Hence the magnification of the measurement error, in units of the magnification of the magnitude of the oscillatory signal, is e_k/F_k . That quotient depends on the nature and location of the acoustic glitch and the central frequency of the contributing modes, through F_k , and, through d_{kl} , on the order k of the difference. It is tabulated in Table C1 for the HeII ionization zone and for the base of the convection zone, at the median frequency $\nu_n = 2.75 \text{mHz}$ and the two extreme frequencies 1.5 and 4.0 mHz. For the HeII ionization zone the signal amplitude factor F_k is augmented by a factor of about 1.4 when k is increased by unity, but that is more than offset by the augmentation, by a factor of about 1.9, of the error magnification e_k . Choosing which order k of the differ-

ence to adopt must therefore require a tradeoff between the value of the error quotient e_k/F_k and the degree of difficulty in separating the smooth and oscillatory components. It is interesting to note that at the base of the convection zone e_k/F_k is lowest for $k = 2$ (except, marginally, at the lowest frequency), although not greatly so, which perhaps favours $\Delta_2\delta\nu$ as a diagnostic, in accord with the conclusion of Ballot et al. (2004) drawn from Monte Carlo calculations.

APPENDIX D: EVALUATION OF THE CONVECTION-ZONE DISCONTINUITY

The difference equations that were used to represent the differential equations of stellar evolution (which are based simply on second-order-accuracy centred differences in space and time on a fixed Lagrangian spatial mesh) do not adequately account for the mathematical properties of the structure in the vicinity of the base of the convection zone. The convective heat flux was computed from a local mixing-length formalism with a mixing length set to a constant proportion of a pressure scale height (which therefore does not vanish at the edge of the convection zone), which leads to a discontinuity in the second spatial derivative of the density, and hence, according to equation (B4), in the critical cutoff frequency, which, as is common, was implicitly presumed to be absent when adopting the difference equations for the computations. Therefore particular care should be taken when estimating conditions at the base of the convection zone for the purpose of determining the parameters τ_c and A_c in the seismic signature. Perhaps the most straightforward way to have computed the structure would have been to ensure that there was always a mesh point at the base of the convection zone and to tailor the difference scheme either side of that point to accommodate the correct mathematical structure of the solutions. But the models had already been computed, and so it was necessary instead to fit appropriate functional forms to the solutions close, but not too close, to the base of the convection zone for the purpose of evaluating the magnitude of the discontinuity.

The functional forms adopted were those derived by Christensen-Dalsgaard, Gough & Thompson (1991). Above the base of the convection zone, $r = r_c$, the density variation is smooth, and a polynomial extrapolation of $d \ln \rho / dr$ and $d^2 \ln \rho / dr^2$, the latter of which was calculated by numerical differentiation, to $r = r_c$ is adequate. For $r < r_c$ we fitted to $d \ln \rho / d \ln r$ the function

$$-\frac{R}{\Lambda h r} z^{-h} \left[1 + \frac{(u-h)q}{h} z^{-u} + \frac{(2u-h)y}{h} z^{-2u} \right]^{-1}, \quad (\text{D1})$$

in which $z = \rho / \rho_0$ and

$$\Lambda = \frac{f p_c}{h \rho_c} \frac{R}{GM} \left(\frac{\rho_c}{\rho_0} \right)^h \quad (\text{D2})$$

with $p_c = p(r_c)$, $\rho_c = \rho(r_c)$; also $f = (4 + \lambda + v) / (3 + \lambda)$, $h = f - 1$, $q = \lambda h w / (1 + \lambda f)$, $y = (1 + 2\lambda)(f + \lambda w) h w / [2(2\lambda f + f + 1)]$, $u = (1 + \lambda)f$, $w = 1 / (3 + v)$, ρ_0 being an integration constant to be determined in the fitting process, where formally $\lambda = (\partial \ln \kappa / \partial \ln \rho)_\vartheta$ and $v = -(\partial \ln \kappa / \partial \ln \vartheta)_\rho$ are the logarithmic partial derivatives of opacity κ with respect to density ρ and temperature ϑ , both derivatives being evaluated at $r = r_c$. Expression (D1) was fitted by least squares

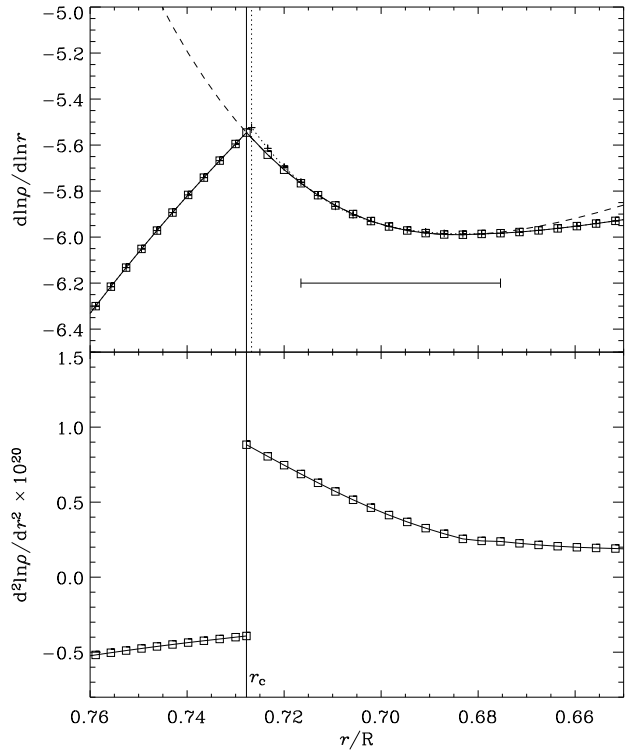


Figure D1. Density derivatives near the base of the convection zone. The top panel shows the first derivative of density. The plus symbols display the density derivatives of the original (unmodified) model and are connected by the dotted curve. The vertical dotted line indicates the location of the base of the convection zone of the unmodified model. The dashed curve is the result of fitting the analytical expression D1 by least squares to the plus symbols of the original (unmodified) model within the fitting domain indicated by the horizontal solid line. The square symbols show the density derivatives of the modified model and are connected by the solid curve (they lie on the dashed curve above the mid-point of the fitting domain, and on the dotted curve below it). The vertical solid line indicates the new location of the base of the convection zone, r_c . The bottom panel shows the result for the second density derivatives of the modified model obtained by numerical differentiation.

to the solar models in the region indicated in Fig. D1 by adjusting the parameters Λ , ρ_0 , λ , and v , the outcome of which is illustrated as the dashed curve in the upper panel of the figure for the central model 0. Its intersection with the extrapolation of $d \ln \rho / d \ln r$ in the convection zone determines r_c , from which it can then be confirmed that equation (D2) is satisfied. From this can be computed the second derivative of $\ln \rho$, which is illustrated in the lower panel of Fig. D1, and hence the discontinuity $d^2 \ln \rho / dr^2|_{r_{c+}} - d^2 \ln \rho / dr^2|_{r_{c-}}$ which is needed for evaluating A_c according to equation (18). Both A_c and $\tau_c = \tau(r_c)$ of the nine test models are plotted against Y in the first lower two panels of Fig. 4.